The Structural and Electronic Properties of Amorphous Ge and its Alloys(Dissertation_全文)

AUTHOR(S):

Tamura, Kozaburo

学位申請論文

田村剛三郎

The Structural and Electronic Properties of Amorphous Ge and its Alloys

A Thesis

Presented to the Faculty Of Science

Kyoto University

by

Kozaburo Tamura

1973

Preface

The structure and electronic properties of amorphous Ge are quite different from those of liquid Ge, which is densely packed, has the octahedral local environments rather than tetrahedral and exhibits a metallic behavior.

Therfore it is interesting to investigate the physical properties of amorphous Ge by applying pressure.

It is found that the semiconductor to metal transition occurs at pressure of 60 Kbar in amorphous Ge. The transition pressure is changed by addition of Sn. The atomic arrangem of amorphous Ge-Sn alloys are tetrahedral with a random nea est neighbour environment.

Effect of pressure on amorphous Ge-Ni alloys was studied. Semiconductor to metal transition occurs in the concentration range below 30 at.% Ni at almost the same pressure as in amorphous Ge. Amorphous Ge-Ni alloys with over 30 at.% Ni concentration show metallic properties.

X-ray scattered intensity curves for amorphous Ge-Ni alloys in the concentration range over 30 at.% Ni show quite similar pattern with those for liquid.

The investigations of the systematic variation of atomic and electronic structure of such amorphous alloys with concentration and also the extent of the similarity of physical properties in these amorphous alloys with those in liquid state are interesting.

The valence band spectra of amorphous Ge-Ni, Ge-Fe and Ge-Au alloys are investigated by means of X-ray photo-electron

emission. The shape and position of the peak in the spectrum associated with d-state change with concentration.

This thesis contains three parts as follows

Part I : Nonmetal to Metal Transition in Amorphous Ge and Ge-Sn Alloys under High Pressure

Part II : Effect of Pressure on the Electronic Properties of Amorphous Ge-Ni Alloys

Part III : X-ray Photoemission Spectra of Valence Bands in Amorphous Ge-Ni, Ge-Fe and Ge-Au Alloys

Part 1

Non-Metal to Metal Transition in Amorphous C and Ge-Sn Alloys under High Pressure

§1 Introduction

There has been many experimental and theoretical investigations[1] on the properties of amorphous Ge because it is the most typical example of amorphous semiconductors. The structure of amorphous Ge has been investigated by X-ray and electron diffraction experiments.[2~4] The radial distribution function deduced from the diffraction data shows that the atoms in the amorphous Ge are surrounded by a tetrahedron of other atoms with an average separation similar to that in the crystalline Ge. Several models[5~7] for the structure of amorphous Ge have been proposed on the basis of these results. The microscopic structures, for example, the existence of vacancies, voids and dangling bonds etc. have been studied by means of the measurements of the density,[8,9] small angle scattering of electron diffraction[10] and ESR.[11] However the definite picture for the structure of amorphous Ge seems to be unknown at present. It should be also noticed that the structural and electronic properties of amorphous Ge are quite different from those of liquid Ge which is densely packed with the octahedral local environments rather than tetrahedral and exhibits a metallic behavior.[12] This is in contrast to the fact that the amorphous metal and alloys produced by several methods behave like the corresponding liquid state in the structural and electronic properties.[13]

The picture of conduction mechanism in amorphous semiconductor has become clearer by various experimental and theoretical efforts. The conduction process contains intrinsic and extrinsic conductions over the whole temperature range. At high temperature the

intrinsic conduction is dominant and it appears with a large activation energy. As Stuke[14] has emphasized for many amorphous semiconductors the plot of logarithmic conductivity against reciprocal temperature gives a good straight line as same as for crystalline semiconductor. At low temperature the extrinsic conduction becomes dominant. Extrinsic conduction is caused by the hopping of the localized electrons in the band tail or in the vicinity of the Fermi level. A large number of as-deposited films show a $T^{-\frac{1}{4}}$ law dependence of the conductivity up to room temperature and even above, as suggested by Mott.[15] This seems to suggest that the hopping in the localized states near the Fermi level is dominant. Furthermore the tunneling experiments support this situation.[16] If hopping conduction or phonon assisted tunneling conduction really exists, which is one of the most important feature in amorphous semiconductor, it is interesting to investigate the effect of pressure on this conduction mechanism. The hopping mobility can be expressed as follows;[17]

$$\mu = (e\nu_{ph} d^2 \phi/kT)\, e^{-Ed/kT}\, e^{-2\alpha d} \quad ,$$

where ν_{ph} is an average optical phonon frequency, ϕ is a constant, Ed is the hopping activation energy, α gives the rate of fall-off of the localized wave functions, and d is the average interatomic separation. Therefore it is to be expected that the mobility increases very rapidly with decreasing d unless the wave functions are spread out.

Since the density, structure and electronic properties of amorphous Ge are quite different from those of liquid Ge, it is interesting to investigate the physical properties of amorphous

Ge by compression. The investigation on the change of mobility gap or hopping conduction process with pressure is also important. The measurement of resistivity as a function of pressure up to 28 kbar has been reported by Camphansen et al.[18] for the various amorphous Ge prepared by the electrolytic, evaporation and sputtering method, and for those annealed at 153°C.

In this paper we report the effect of pressure on the electrical resistance of amorphous Ge and Ge-Sn alloys under high pressure up to 130 kbar.

§2 Experimental Procedure

2-1 Preparation of Samples

Amorphous Ge and its alloy films were prepared by evaporation onto the mica substrates kept at or below room temperature under vacuum better than 10^{-6} torr. The vacuum was kept below $1 \sim 2 \times 10^{-6}$ torr during evaporation.

The sample was evaporated from the basket of the tungsten filament with 0.3 mm in a diameter which was outgassed carefully under vacuum. The distance between the tungsten filament and the substrate was about 10 cm. The rates of deposition were about 500 Å/min and the evaporations were performed about every one minute at 10 minutes intervals in order to prevent the heating up of the substrate due to the radiation from the filament as possible.

The small pellets of Ge or Ge-Sn mixture with about 2 mm in a diameter were dropped one by one into the basket of tungsten filament through the guide of stainless tube under vacuum, and then evaporated. It is well known that two constituents, Ge and Sn are competely soluble in the liquid state but dissoluble in the solid state in almost the whole concentration range. Therefore the Ge-Sn alloys melted in a evacuated quartz tube were rapidly quenched into water in order to obtain the homogeneous alloy pellets. The mica substrates shaved and cut from mica sheets were of 20 μm or more thickness and 1 mm square. The films of Ag and Au with 5000 Å thickness deposited on the mica substrate were used as the electrodes which were kept 0.1 mm apart from each other. The sample was deposited on the substrate through the mask with a slit of 0.1 mm in width which was put on the substrate. The thickness

of samples used for the present measurement were usually 1~2 μm. The dimensions of samples on the mica substrates are shown in Fig. 1 schematically.

2-2 Apparatus

For measurements of electrical resistance at high pressure up to 130 kbar, pressure was applied at room temperature by an opposite anvil type apparatus developed by Balchan and Drickamer[19] using an external hydraulic press. A pyrophyllite pellet of the appropriate size and shape with 0.33 mm in a center thickness and 3.00 mm in diameter was used for pressure medium. After pre-compression the center flat area of the pyrophyllite pellet was removed with a drill and then the pyrophyllite ring into the center was inserted. The schemeatic diagram of the center assembly are shown in Fig. 2, in order to make clear the situation of sample geometry. The electrical contacts were made through the thin copper sheets connecting between the cemented tungsten carbide anvils and the electrodes of film on the mica substrate.

2-3 Calibration and Measurement of Resistance

The electrical resistance was measured by detecting the changes of potential across the sample caused by a small constant direct current. The voltage and current probes were soldered to the outside of steel jackets of the two anvils. Pressures were determined by the fixed points of Bi(I-II), Bi(IV-V) and Pb(I-II) transitions at 25.4, 77 and 130 kbar. It should be noticed that the pressures generated in AgCl medium are sensitively affected by the geometrical arrangements for all the parts of high pressure

cell. The error of calibrations was about 10 %. To decide the pressure more precisely we measured the parallel resistance of the sample and Bi film with about 1 μm thickness deposited just on the film of the sample . A typical example for the measurement is shown in Fig. 3. In the present experiments, the sharp transition from non-metal to metal of samples took place at pressure between the two fixed calibration points of Bi. Therefore it was possible to decide the transition pressure within the error of 1~2 %. The copper-constantan thermocouple was inserted into near the sample through the hole of the side jacket to measure the temperature of the sample.

§3 Results and Discussion

3-1 Pure Ge

Fig. 4 shows the electrical resistance versus pressure curves of amorphous and polycrystalline Ge. The polycrystalline Ge was obtained by annealing the amorphous film at 500°C under vacuum for an hour. It was ensured for the film annealed at 500°C to show the crystalline lines indexed as a diamond type structure from the X-ray diffraction measurement.

On increasing pressure, the electrical resistance of the polycrystalline film gradually increases up to about 50 kbar and then decreases. It suddenly drops at pressure of 100 kbar which is nearly the same as the previous data for crystalline Ge observed by Minomura and Drickarmer [20] On the other hand the pressure dependence of the resistance in the amorphous Ge is very different from the crystalline Ge. The resistivity of amorphous Ge is estimated to be $3\times10^{2}\Omega$-cm at atmospheric pressure. It slightly increases up to about 10 kbar and rapidly decreases by a factor of 6~7. Then, it drops sharply down to about 2×10^{2} $\mu\Omega$-cm at 60 kbar and the second drop down to $2\sim3\times10$ $\mu\Omega$-cm appears at about 100 kbar which corresponds to that observed for the polycrystalline films. It is noticed that the resistance changes very little with pressure in the range of pressure between 60 and 100 kbar.

The pressure dependence of the resistance in the amorphous Ge was precisely measured in the low pressure region by using Cu-Be pressure bomb. Fig. 5 shows the result for the pressure dependence of the resistance in amorphous Ge up to 10 kbar, where the value of resistance is normalized by that at atmospheric

pressure. Paul and Brooks[21] have measured the change of the resistance of crystalline Ge with pressure up to 30 kbar. Their result is also shown in Fig. 5. It is noticed that the pressure derivative of resistance $\frac{d \ln R}{d p}$ for as-deposited amorphous Ge is 4.0×10^{-2} kbar^{-1} which is much smaller than that for crystalline Ge. Recently Camphausen et al.[18] have reported measurements of resistance as a function of pressure up to 28 kbar for amorphous Ge prepared by the three different methods and also annealed at 153°C. Our data for amorphous Ge is in good agreement with their result of unannealed sputtered Ge. They have shown that the variation of resistance with pressure for the annealed amorphous sample is very different from that for the unannealed amorphous samples. The logarithmic resistance versus pressure curves of annealed amorphous samples give a good straight lines and their pressure derivative $\frac{d \ln R}{dp}$ are almost the same as that of crystalline Ge. Another important aspect is that the pressure coefficients of the optical gap, which essentially gives the electrical gap of the intrinsic conduction, are positive and almost the same for annealed and unannealed amorphous samples in spite of the fact that the pressure coefficients of resistance are quite different each other. Therefore it is not unreasonable assumption that the extrinsic conduction is predominant for the transport mechanism in as-deposited amorphous Ge compared to that in crystalline Ge.

The temperature dependence of resistance in amorphous Ge under pressure and the pressure dependence of activation energy

are shown in Fig. 6 and Fig. 7 respectively. The activation energy in Fig. 7 deduced from the derivative of logarithmic resistance versus reciprocal of temperature near room temperature does not represent the intrinsic activation energy. It must be thought that the extrinsic conduction process is still dominant in this temperature region, which has been studied by many investigators at atmospheric pressure. The amorphous Ge exhibits semiconducting behaviour up to 60 kbar. It is considered that Ge sample shows metallic behaviour under the pressure between 60 and 100 kbar, since the resistance gradually decreases with falling temperature and the sample becomes superconductor near $5^{o}K$.[22] The sample under pressure over 100 kbar is metallic and the temperature coefficient of resistance is small but positive as shown in Fig. 8.

For the Ge sample under pressure between 60 and 100 kbar, the sharp lines corresponding to crystalline structure could not be detected in X-ray diffraction pattern. But the determination of the definite structure at high pressure has not yet been successful. The recent work[23] of amorphous Si under high pressure has revealed that semiconductor to metal transition occurs at the pressure of 100 kbar which is much lower than that observed for crystalline Si, as same as in the case of amorphous Ge. On decreasing pressure the resistance recovers to the same value before compression, and the aspect of the resistance-pressure curve is reproducible by repeating the application and release of pressure. After releasing pressure the sample in the metallic phase recovers to semiconductor, however, the X-ray diffraction measurement shows that the sample has an amorphous structure. This evidence encourages

us to believe that the Ge sample under pressure between 60 and 100 kbar is amorphous. The X-ray pattern of the sample released back from the pressure below the first transition point to atmospheric pressure has been just the same as that of amorphous Ge at normal pressure. However the samples released back from the pressure between 60 and 100 kbar were crystallized. X-ray diffraction lines of the sample released from the pressure of about 80 kbar could be indexed for that of the same diamond structure as crystalline Ge, while the sample released from the pressure above 100 kbar shows the tetragonal structure. Bundy and Kasper[24] have found that the tetragonal Ge consisted of linkages of rather distorted tetrahedra can be formed when crystalline Ge with diamond structure is compressed over 100 kbar and then released back to atmospheric pressure. The sample under pressure over 100 kbar may have β-Sn type structure[25] since the transition pressure coincides to that of crystalline Ge and also the structure of the sample released from over 100 kbar is the same as that of crystalline Ge.

Fig.4 may suggest that 'amorphous' non-metal to 'amorphous' metal transition occurs at the pressure of 60 kbar by application of pressure for amorphous Ge and the transition at 100 kbar, accompanied by the resistance drop by a factor of 2×10^{-1}, is due to the crystallization to β-Sn type structure. Further work by the present authors reveals that the transition pressure of amorphous Ge annealed at 200, 300 and 400°C is the same as that of as-deposite amorphous Ge.

3-2 Amorphous Ge-Sn alloys

In the previous paper[22] we have reported the pressure dependences of the resistances in amorphous Ge-Ni alloys. The sharpness of the transition from non-metal to metal changes with addition of Ni to Ge and it becomes dull, though the transition pressure does not change so much. The change in the character of covalent bonding with addition of Sn to Ge may give a large effect on the optical gap and localization of the carriers with energies near the Fermi level in amorphous Ge. Therefore it is interesting to explore whether the transition pressure changes or not by addition of Sn.

In recent years the studies have been reported an amorphous Ge-Sn alloys by a few authors. S. Sato et al.[26] have measured the temperature dependence of the dc conductivity and the frequency dependence of the ac conductivity at room temperature in Ge-Sn alloy films. They have tried to interpret the results on the basis of pseudo-gap model. The structural and optical properties have been studied in details on these alloy systems with Sn concentration 0, 25, and 50 at.% by R. J. Temkin et al.[27] According to Temkin et al. the minimum optical gap decreases with increasing Sn content.

Fig. 9 shows the intensity patterns of X-ray diffraction without any correction for amorphous Ge-Sn alloys. The variation of the diffraction patterns with increasing Sn concentration is quite different from those of amorphous Ge-Ni alloys.[22] The atomic arrangement is found to be tetrahedral with a random nearest neighbour environment. Temkin et al. have studied the

structural properties of amorphous Ge-Sn alloys in more details. The radial distribution function shows that the mean separation between Ge atoms slightly increases with Sn concentration.

Fig. 10 shows the pressure dependences of resistances in Ge-Sn alloys in the range of concentration less than 10 at.% Sn. The resistivity does not change so much with Sn concentration at atmospheric pressure and at room temperature. It could be seen that the sharp transitions from non-metal to metal exist in these concentration range and change with addition of Sn. The resistances decrease with increasing pressure nearly in the same way as that of pure amorphous Ge and the transition pressure increases with increasing Sn content. The change of the transition pressure with increasing Sn content was precisely determined by using the method mentioned in §2 and it is shown in Fig. 11. Recently it has been found that the transition pressure changes remarkably by the addition of Si to Ge and it increases by 20 kbar by the addition of 10 at.% Si content. It will be published later in detail

The measurements of X-ray diffraction, Hall coefficient, thermopower, optical properties etc. at various temperatures under high pressure will be helpful for understanding the nature of non-metal to metal transition in amorphous Ge and Ge-Sn alloys.

References

(1) See, for example
N.F.Mott and E.A.Davis; Electronic Process in Non-Crystalline Materials, Oxford (1971)
D.Adler; Amorphous Semiconductor CRC Press London (1971)

(2) H.Richter and O.Fürst; Z.Naturforsch 6a (1951) 38

(3) H.Richter and G.Breitling; Z.Naturforsch 13a (1958) 988

(4) N.J.Shevchik and W.Paul; J.Non-Crystalline Solids 8-10 (1972) 381

(5) T.B.Light and C.N.J.Wagner; J.Appl.Cryst. 1 (1968) 199

(6) R.Grigorovici and R.Manaila; J.Non-Crystalline Solids 1 (1969) 371

(7) D.E.Polk; J.Non-Crystalline Solids 5 (1971) 365

(8) A.H.Clark; Phys.Rev. 154 (1967) 750

(9) T.B.Light; Phys.Rev.Letters 22 (1969) 999

(10) S.C.Moss and J.F.Graczyk; Phys.Rev.Letters 23 (1969) 1167

(11) M.H.Brodsky and R.S.Title; Phys.Rev.Letters 23 (1969) 581

(12) S.P.Isherwood, B.R.Orton and R.Manaila; J.Non-Crystalline Solids 8-10 (1972) 691

(13) A.K.Sinha; Phys.Rev. (B) 1 (1970) 4541

(14) J.Stuke; J.Non-Crystalline Solids 4 (1970) 1

(15) E.A.Davis and N.F.Mott; Phil.Mag. 22 (1970) 903

(16) J.W.Osmun and H.Fritzsche; Appl.Phys.Letters 16 (1970) 87

(17) N.F.Mott; Phil.Mag. 19 (1969) 835

(18) D.L.Camphausen, G.A.N.Connell and W.Paul; J.Non-Crystalline Solids 8-10 (1972) 223

(19) A.S.Balchan and H.G.Drickamer; Rev.sci.Instrum. 32 (1961) 308

(20) S.Minomura and H.G.Drickamer; J.Phys.Chem. Solids 23 (1962) 451

(21) W.Paul and H.Brooks; Phys.Rev. 94 (1954) 1128

(22) K.Tamura, J.Fukushima, H.Endo, S.Minomura, O.Shimomura and K.Asaumi; Proc. of 2nd International Conference of the Properties of Liquid Metal, Tokyo, 1972 (Taylor and Francis), p 295

(23) S.Minomura; Private Communication

(24) F.P.Bundy and J.S.Kasper; Science 139 (1963) 340

(25) J.C.Jamieson; Science 139 (1963) 762

(26) S.Sato, N.Yamaguchi and H.Ozaki; J.Phys.Soc.Japan 33 (1972) 1497

(27) R.J.Temkin, G.A.N.Connell and W.Paul; Solid State Communications 11 (1972) 1591

Figure Captions

Fig. 1. Dimensions of sample deposited on the mica substrate used for measurement of electrical resistance at high pressure.

Fig. 2. Center assembly of high pressure cell.

Fig. 3. A typical example for the measurement of parallel resistance of sample and Bi films. Transition pressure of sample is decided precisely with respect to the two fixed points of Bi.

Fig. 4. Electrical resistance versus pressure curves for amorphous and polycrystalline Ge films. Polycrystalline films is obtained by annealing amorphous film at 500°C.

Fig. 5. The normalized resistance versus pressure for amorphous and crystalline Ge. The result of crystalline Ge is taken from the data by Paul and Brooks.[21]

Fig. 6. Temperature dependence of resistance of amorphous Ge near room temperature at pressure of 30, 45 and 60 kbar.

Fig. 7. Pressure dependence of activation energy deduced from the derivative of log resistance versus reciprocal of temperature shown in Fig. 6.

Fig. 8. Resistance versus temperature curve near room temperature at pressure of 110 kbar.

Fig. 9. The intensity pattern of X-ray diffraction for amorphous Ge-Sn alloys.

Fig. 10. Resistance versus pressure curves of amorphous Ge-Sn alloys.

Fig. 11. Transition pressure of amorphous Ge-Sn alloys with respect to the Sn content. Transition pressure is determined by the method shown in Fig. 3.

Fig 1

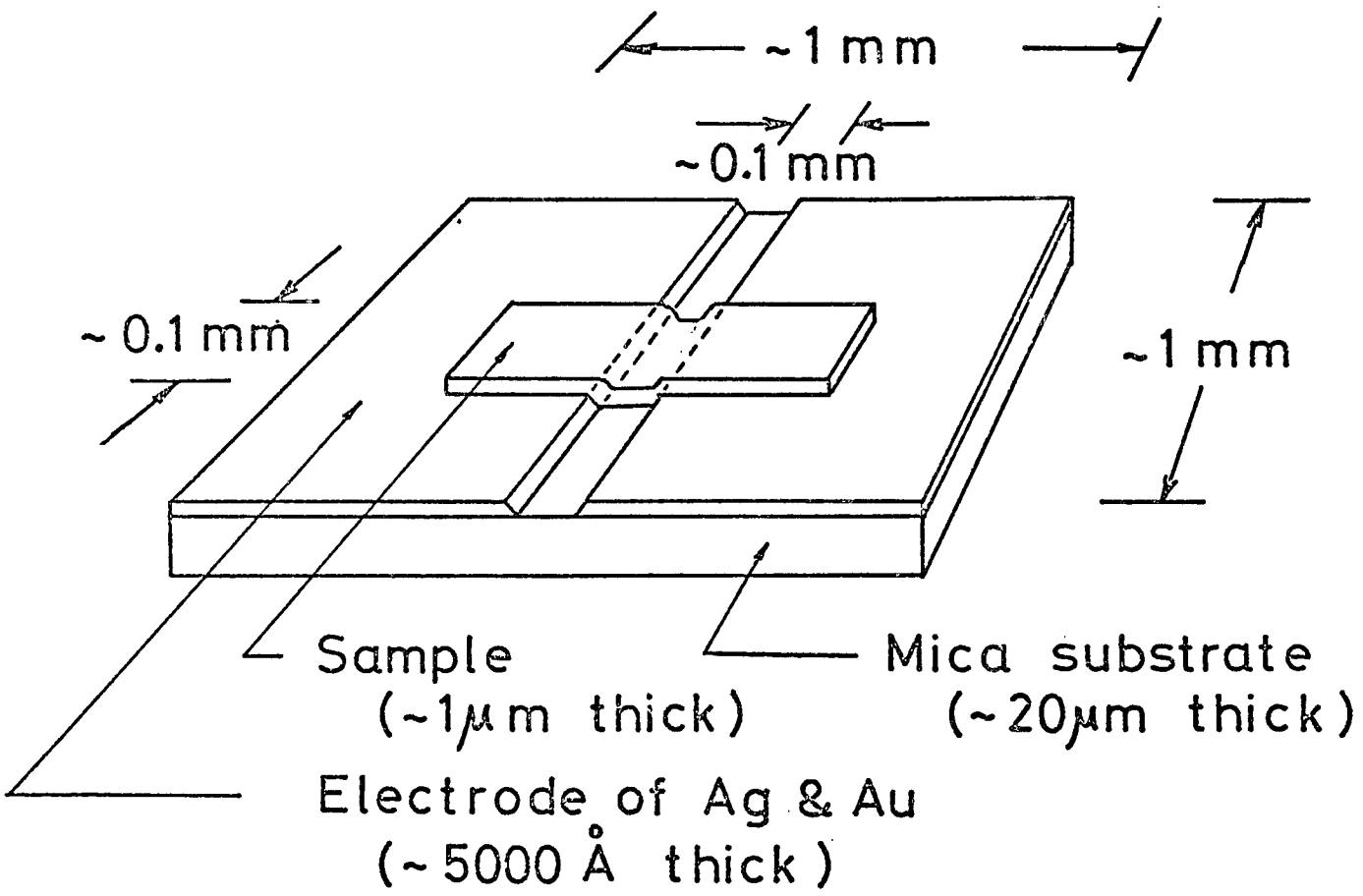
~1 mm
~0.1 mm
~0.1 mm
~1 mm
Sample
(~1μm thick)
Mica substrate
(~20μm thick)
Electrode of Ag & Au
(~5000 Å thick)

Fig 2

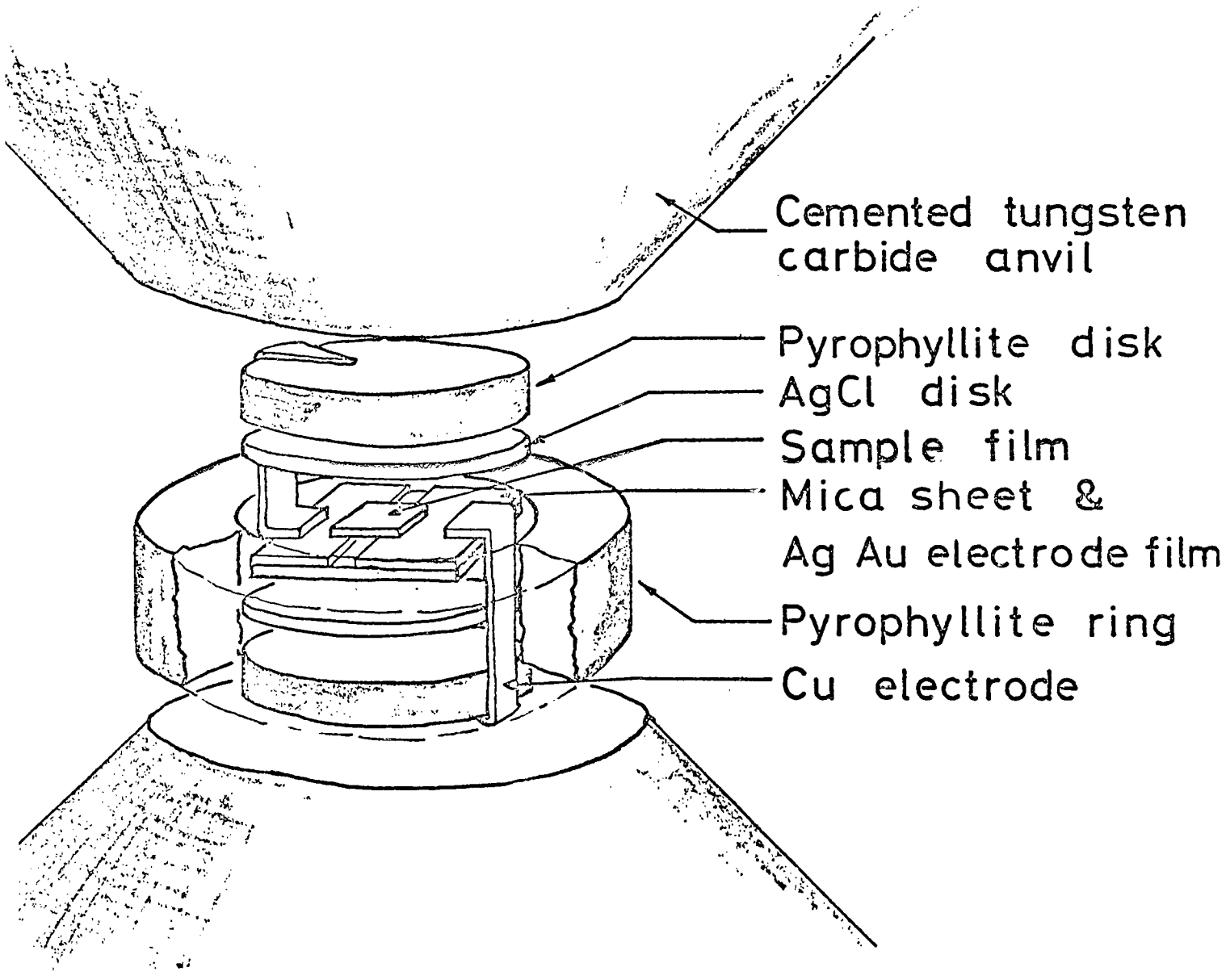
Cemented tungsten carbide anvil
Pyrophyllite disk
AgCl disk
Sample film
Mica sheet &
Ag Au electrode film
Pyrophyllite ring
Cu electrode

Fig 3

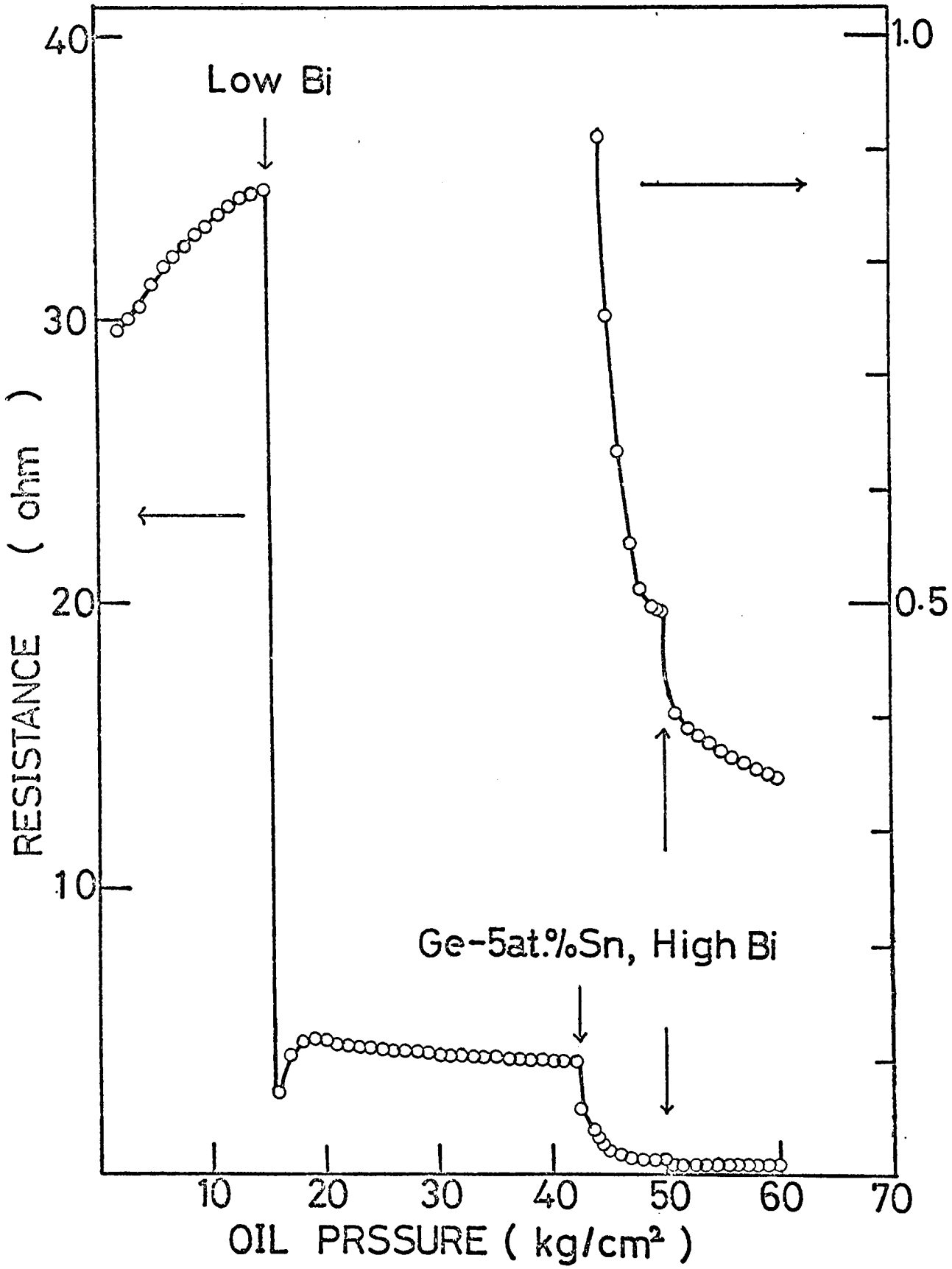
Low Bi
Ge-5at.%Sn, High Bi
RESISTANCE (ohm)
OIL PRSSURE (kg/cm²)
40
30
20
10
1.0
0.5
10
20
30
40
50
60
70

Fig 4

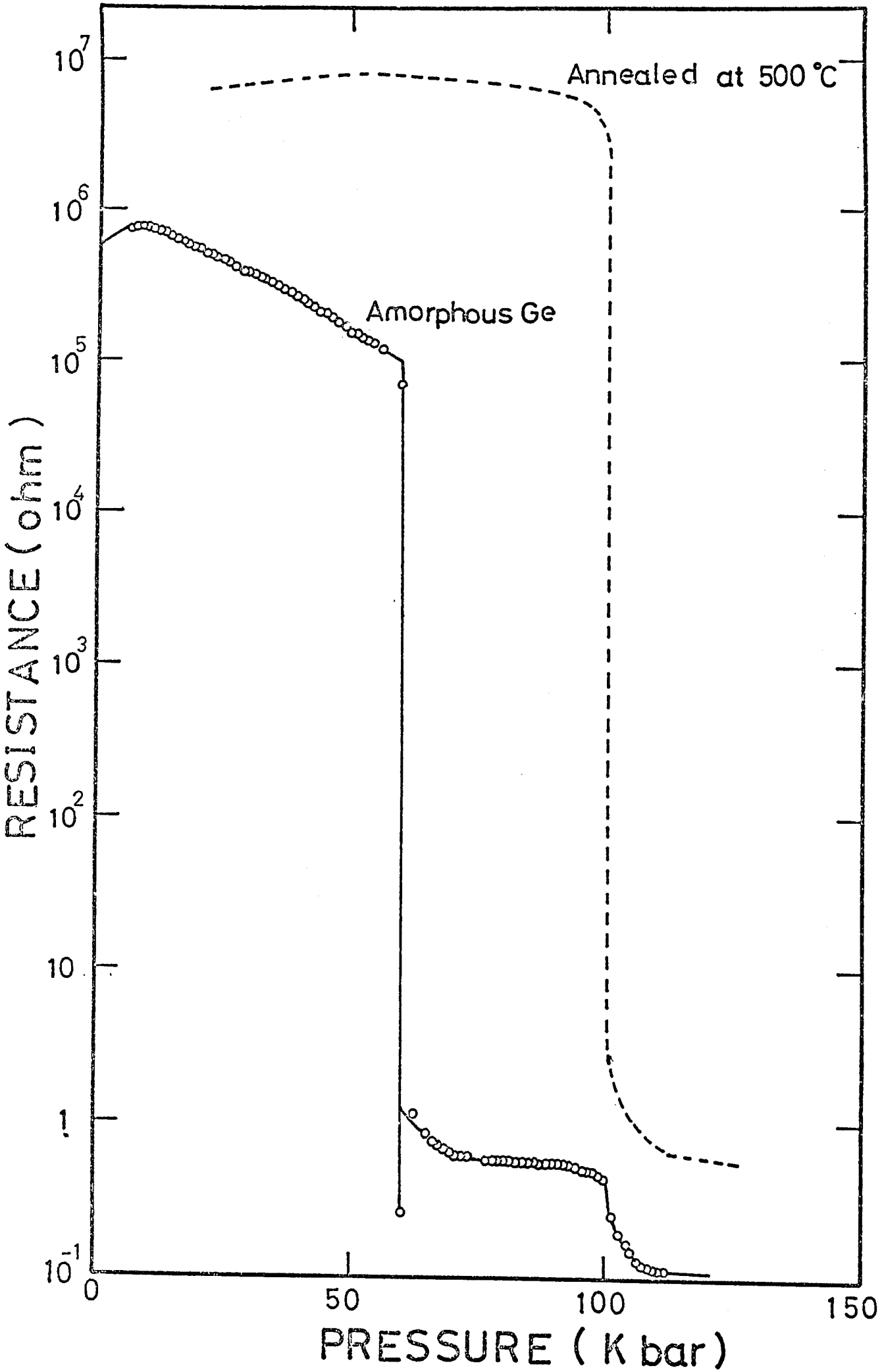
Annealed at 500 °C
Amorphous Ge
RESISTANCE (ohm)
10^7
10^6
10^5
10^4
10^3
10^2
10
1
10^{-1}
0
50
100
150
PRESSURE (K bar)

Fig 5

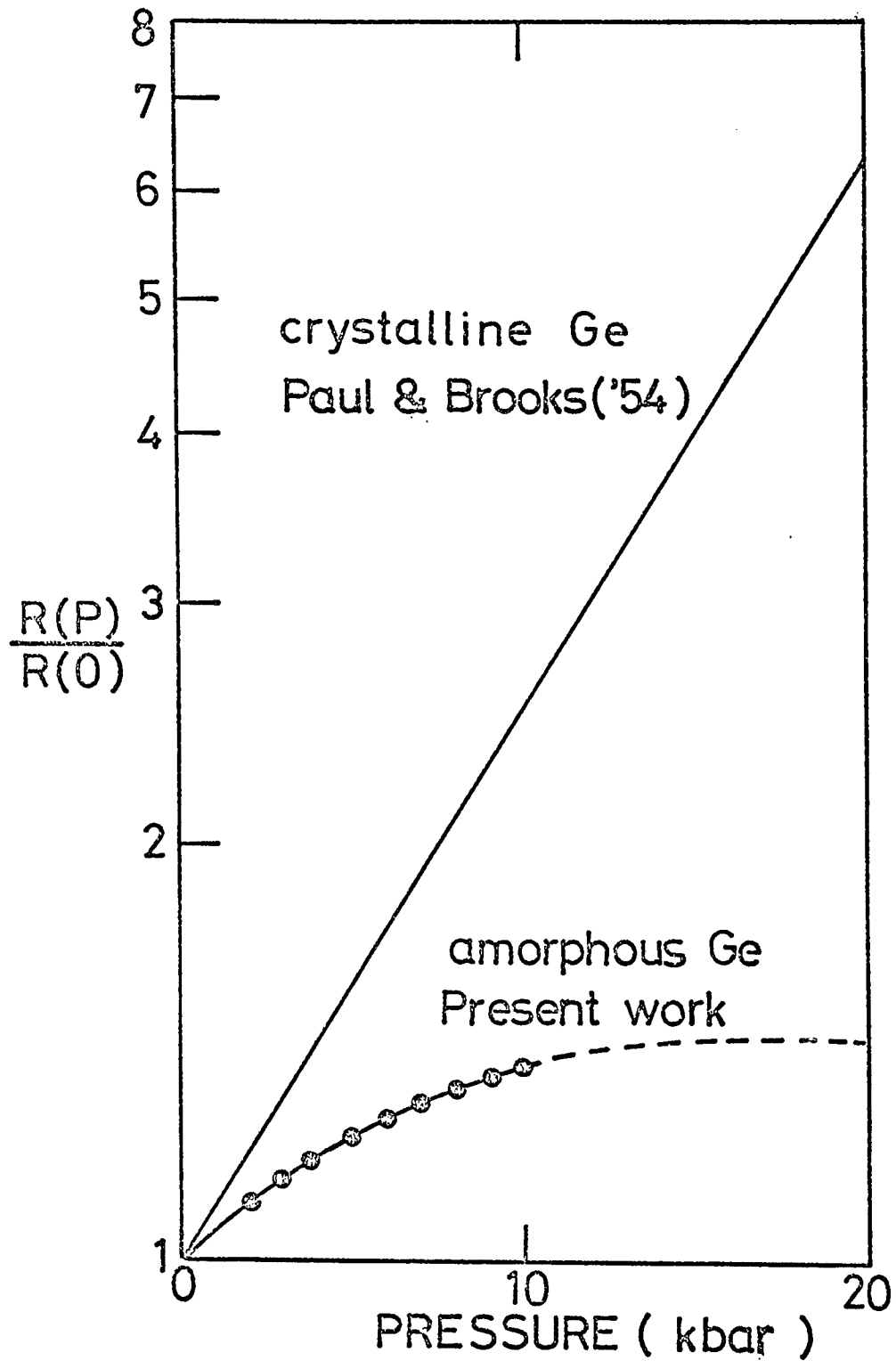
8
7
6
5
4
3
2
1
R(P)
R(0)
crystalline Ge
Paul & Brooks('54)
amorphous Ge
Present work
0
10
20
PRESSURE (kbar)

Fig 6

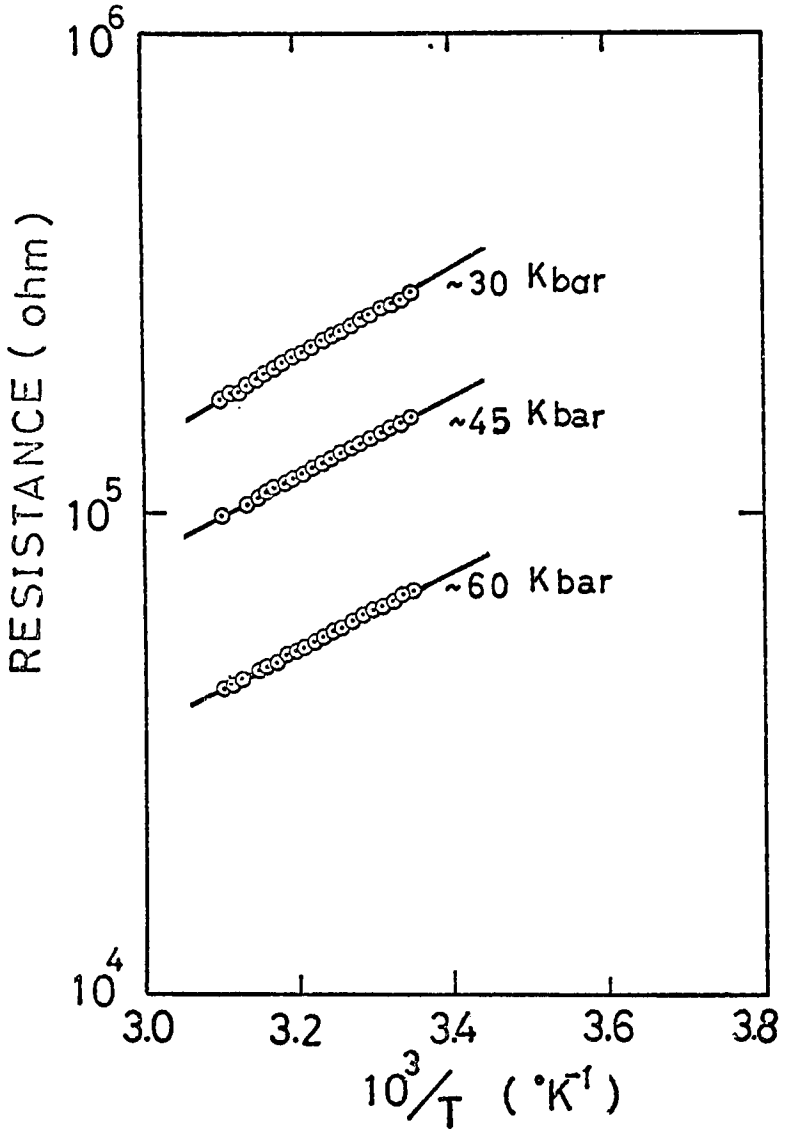
RESISTANCE (ohm)
10^6
10^5
10^4
~30 Kbar
~45 Kbar
~60 Kbar
3.0
3.2
3.4
3.6
3.8
10^3/T (°K^-1)

Fig 7

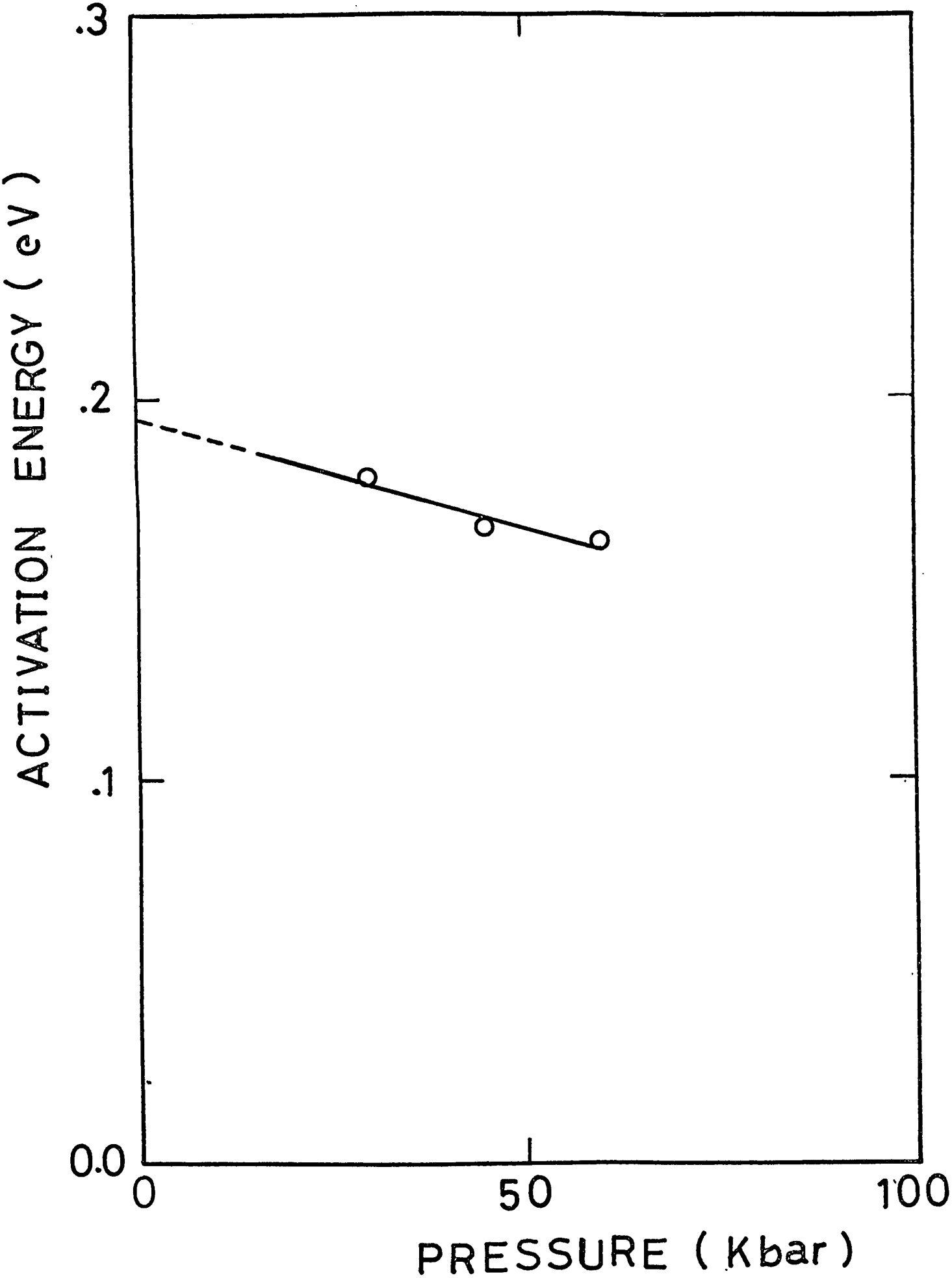

Fig 8

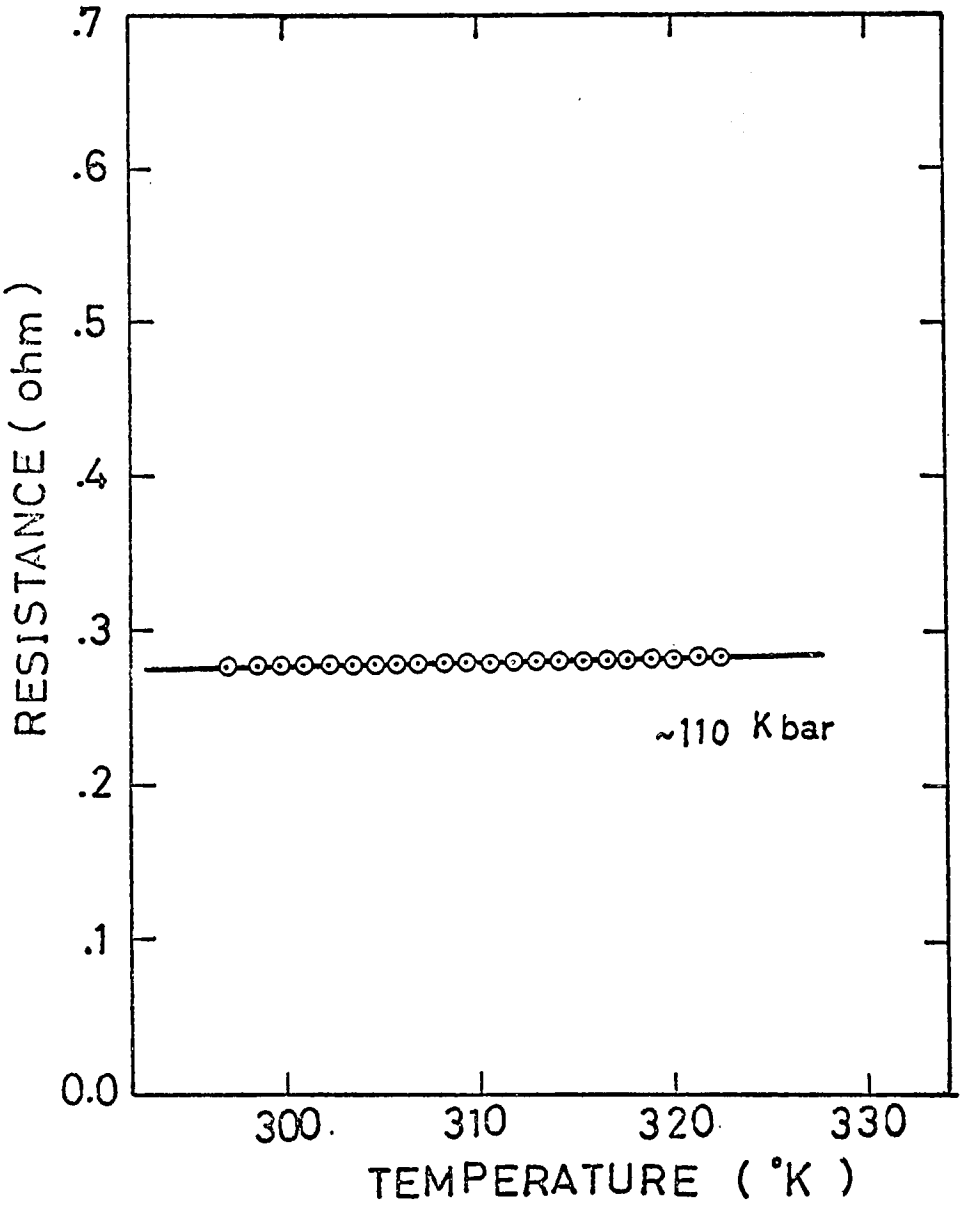
.7
.6
.5
.4
.3
.2
.1
0.0
RESISTANCE (ohm)
~110 K bar
300
310
320
330
TEMPERATURE (°K)

Fig 9

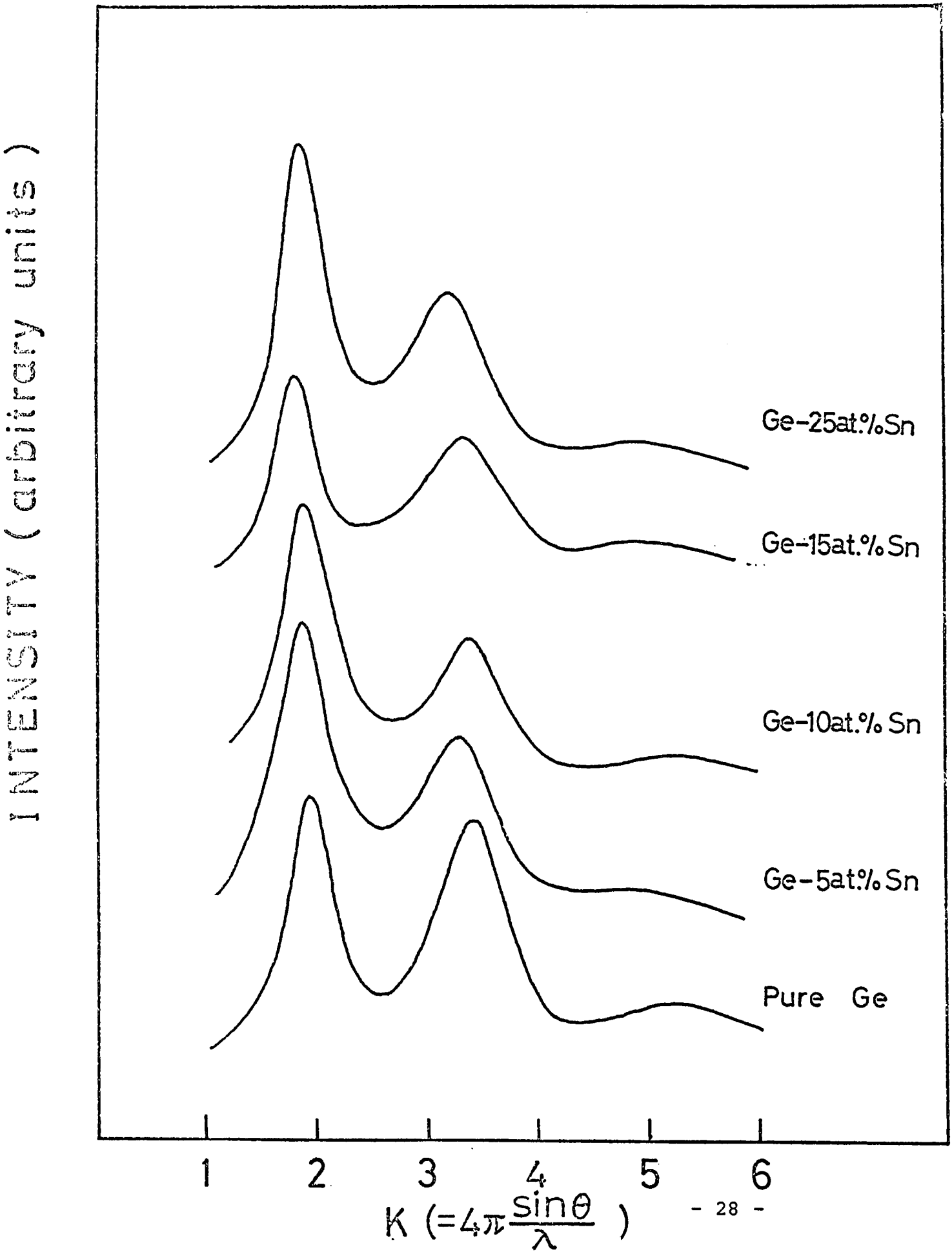
INTENSITY (arbitrary units)
Ge-25at.%Sn
Ge-15at.%Sn
Ge-10at.% Sn
Ge-5at.% Sn
Pure Ge
1
2
3
4
5
6
K (=4π sinθ/λ)

Fig 10

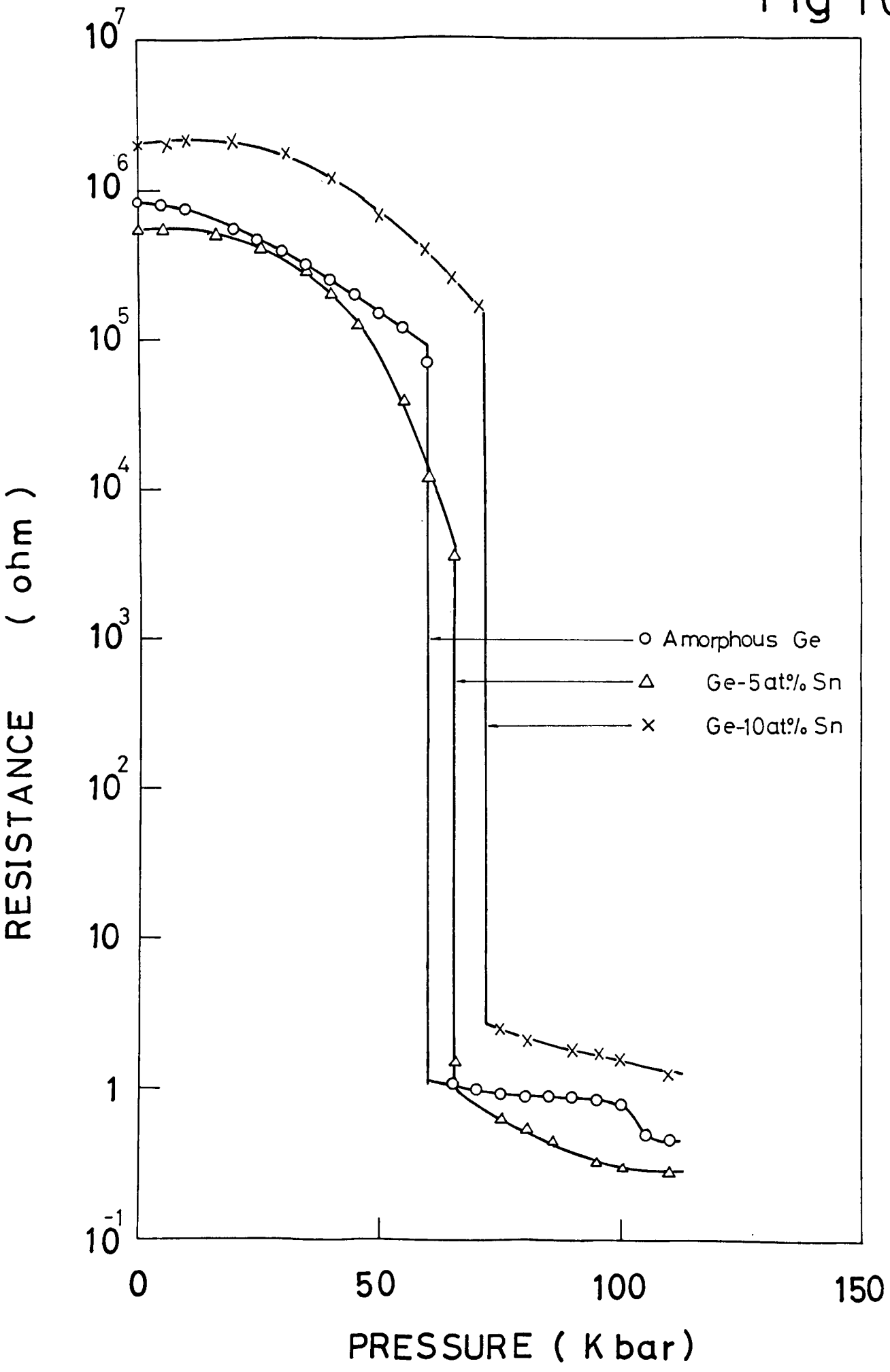
RESISTANCE (ohm)
10^7
10^6
10^5
10^4
10^3
10^2
10
1
10^{-1}
0
50
100
150
PRESSURE (K bar)
o Amorphous Ge
Δ Ge-5at% Sn
× Ge-10at% Sn

Fig 11

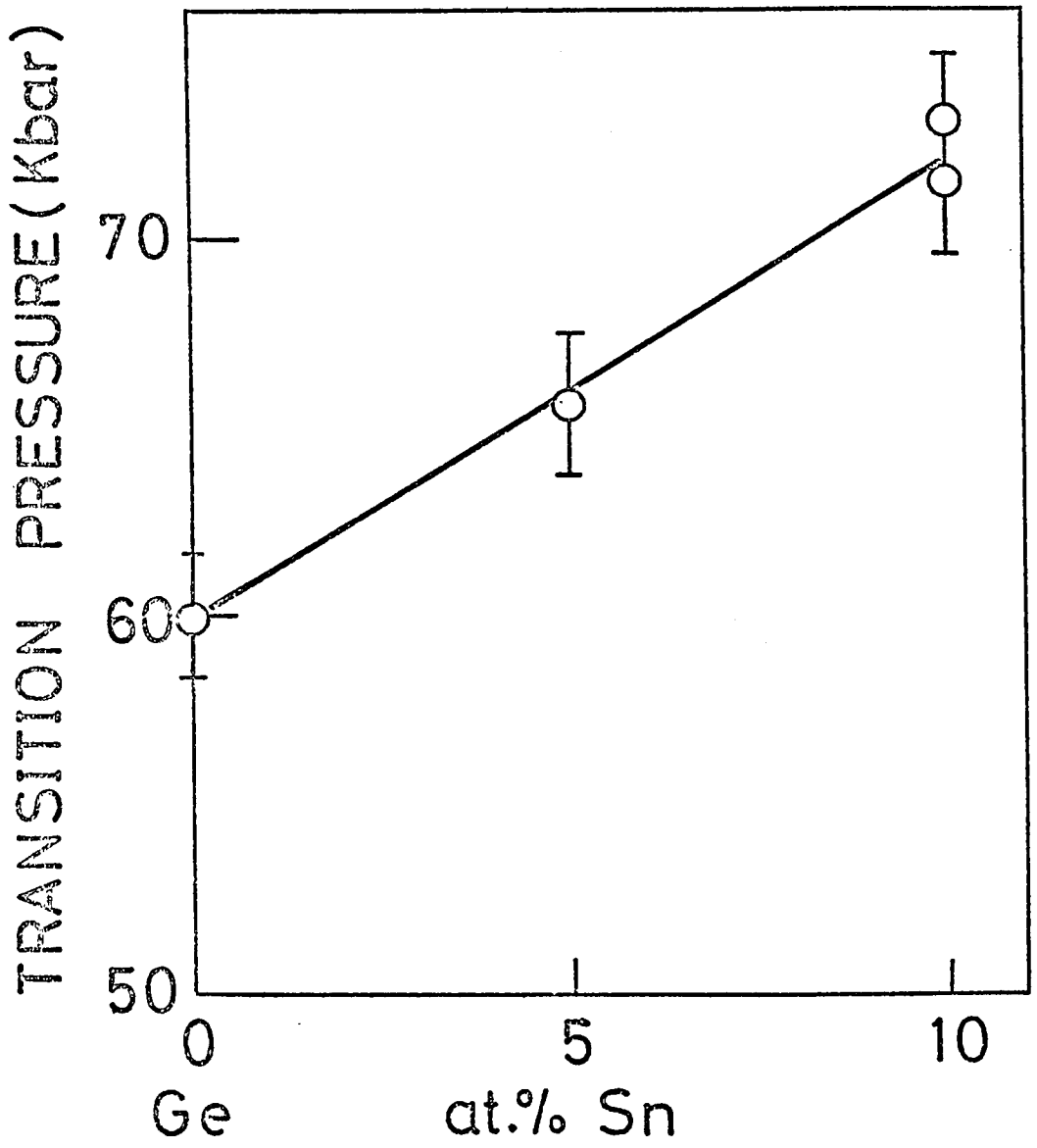

Part II

Effect of Pressure on the Electronic Properties of Amorphous Ge-Ni Alloys

§1. Introduction

The X-ray diffraction patterns (Mader et al 1967) from the amorphous metals and alloys produced by evaporation onto a cold substrate are nearly the same as those observed in a liquid state. There are, however, large differences in the structure and electrical properties between amorphous and liquid Ge. The amorphous Ge behaves like a semiconductor, while liquid Ge like metal. The radial distribution function of amorphous Ge deduced from X-ray measurement shows that the first and second peaks do not appear at the position corresponding to the liquid state. The second peak is relatively high and the coordination number at the nearest neighbour is about 4 (Richter and Breitling 1958) The density of amorphous Ge is approximately 4.8 gr/cm, much lower than that in a liquid phase.

In this paper, we report measurements of X-ray diffraction, density, and X-ray photoelectron spectra for the amorphous phase of Ge-Ni alloys. We report also the variation of electrical resistance with pressure up to 100 Kbar at room temperature for amorphous Ge-Ni alloys in the concentration range to 30 at % Ni, which becomes metallic approximately at 60 Kbar.

§ 2. Experimentals

Amorphous thin films of about 1μm thickness are prepared by condensation in 10^{-6} torr from the mixtures of fine powders of Ge and Ni, rapidly quenched from their melt, onto mica or glass substrates at room temperature, and at liquid N_2 temperature for the maximum concentration of 60 at % Ni.

Pressure are applied at room temperature by an opposed-anvil type apparatus developed by Balchan and Drickamer (1961) Pressures are determined by the fixed point of Bi(1-2) and Bi(3-5) transitions. The density is determined from the weight using microbalance and the thickness using interferometer.

§ 3. Results

X-ray scattered intensity curves I(K) of amorphous Ge-Ni alloys are shown in Fig.1. Intensity of the first peak becomes weaker and the position of the second peak shifts remarkably to a lower value of K with increasing concentration of Ni. It is noticed that I(K) curve in amorphous Ge-40 at % Ni alloy shows quite a similar pattern with liquid Ge-42 at % Ni alloy. Fig.2a shows the pressure dependence of the resistance of amorphous Ge-Ni alloys. In the semiconducting amorphous Ge-Ni alloy, the transitions to metallic states occur at pressure around 60 Kbar, as same as the critical pressure observed in pure amorphous Ge. No discontinuous jump in the resistance in the metallic amorphous Ge-Ni alloys over 30 at % Ni is observed under pressure. The concentration dependence of resistivity of amorphous Ge-Ni alloys at atmospheric pressure and 60 Kbar is shown in Fig.2b. The resistivity of amorphous Ge decreases with increasing concentration of Ni and metallic conductivity with the concentration over 30 at % Ni.

X-ray (Al $K\alpha$) photoelectron spectroscopy is shown in Fig.3 as a function of Ni-concentration. The valence band of amorphous Ge has the single broad maximum in the distribution and the band structure of amorphous Ge is remarkably altered on the addition of Ni. A pronounced peak due to the d electron density of state of Ni appears and intensity of this peak becomes stronger with Ni concentration. The position of the peak corresponding to the d electron density of state of pure Ni shifts toward lower

energy side by alloying. The d spectrum in amorphous Ge-Ni alloys are essentially unchanged with Ni concentration in the range of concentration less than 30 at % Ni, but it shifts gradually with Ni content in large concentration of Ni. The density of state at Fermi energy increases with Ni concentration. The Fermi energy is determined, with a Au sample, as the position where the 6s band is down to half its height. Fig.4 shows the measured density of amorphous Ge-Ni alloys at room temperature the density of amorphous Ge is 4.8 gr/cm and the densities of amorphous Ge-Ni alloys increase rapidly with Ni concentration and approach to the value of the supercooled liquid Ge-Ni alloy down to room temperature in the concentration range over 30 at % Ni, deduced from data for pure liquid Ge and Ni assuming that two constituents are simply mixed each other .

§.4. Discussion and Conclusion

Despite much published literature on the structure of amorphous Ge, it is not fully understood at present. The electronic properties of amorphous Ge depends principally on the local environments of the constituent atoms, i.e., on the first coordination number. The homopolar binding force prevents the formation of a close packed metallic structure. A further increase of average coodination number is achieved by alloying. The alloys are probably significantly more disordered than the pure amorphous Ge. Here is a compositional disorder (Economou et al. 1970) in addition to the lack of long range translational order. In order to satisfy the local valence requirements, the connectivity of the network must change randomly, and local disorder is consequently increased.

It is reasonable to consider the possibility that the addition of Ni may break the covalent bond of amorphous Ge and then the coordination number increases. The measurments of the X-ray diffraction and density exhibits that the structures of amorphous Ge-Ni alloys in the range of Ni concentration over 30 at % is similar with that in the liquid alloy and they become metallic. This suggests that in such alloys the covalent may completely disappear. In such metallic region with dense packing, 4 valence electrons per atom of Ge go into conduction band and 4s electrons of Ni would become non-localized state. The conduction band in Ge-Ni alloy may be built up with a mixing of valence electrons of Ge and Ni. It should be remarked

that the shift of the peak due to the d electron density of state of Ni as seen in Fig.3 reflects the change of Fermi level by alloying (40,50 & 60 at %) In the small concentration range of Ni, where the shift of peak in photoemission spectra is very small with Ni concentration, as shown in Fig.3, the 4s electrons of Ni added to amorphous Ge are extremely localized because of a large number of spatial randomness and the deep potential of Ni. Therefore there is only a very limited sharing of electrons between Ge and Ni. The addition of Ni increases the concentration of broken bonds and the average separation between Ge atoms is reduced. Finally it seems evident that the pressure induced metallic state of amorphous Ge-Ni alloys has a critical density which is equivalent to that of liquid state.

References

Balchan, A.S., and Drickamer, H.G., Rev. Sci. Instr. 32, (1961), 308.

Economou, E.N., Kirkpatrick, S., Cohen, M.H., and Eggarter, T.P. Phys. Rev. Letters, 25 (1970), 520.

Güntherodt, H.J. and Busch, G., Private communication.

Mader, S., Nowick, A.S., and Widmer, H., Acta Metallurgica, 15 (1967), 203.

Richter, H., and Breitling, G., Z. Naturforsh., 13a (1958), 998.

Figure Captions

Fig.1 X-ray scattered intensity curve of amorphous and liquid Ge-Ni alloys.

Fig.2a The pressure dependence of the resistance of amorphous Ge-Ni alloys at room temperature.

Fig.2b The concentration dependence of resistivity of amorphous Ge-Ni alloys at atmospheric pressure (●) and above 60 Kbar (0) Dashed line shows that of liquid state measured by Güntherodt & Busch (1971)

Fig.3 X-ray photoelectron spectra for amorphous Ge-Ni alloys.

Fig.4 The densities at amorphous Ge-Ni alloys at room temperature.

Fig 1

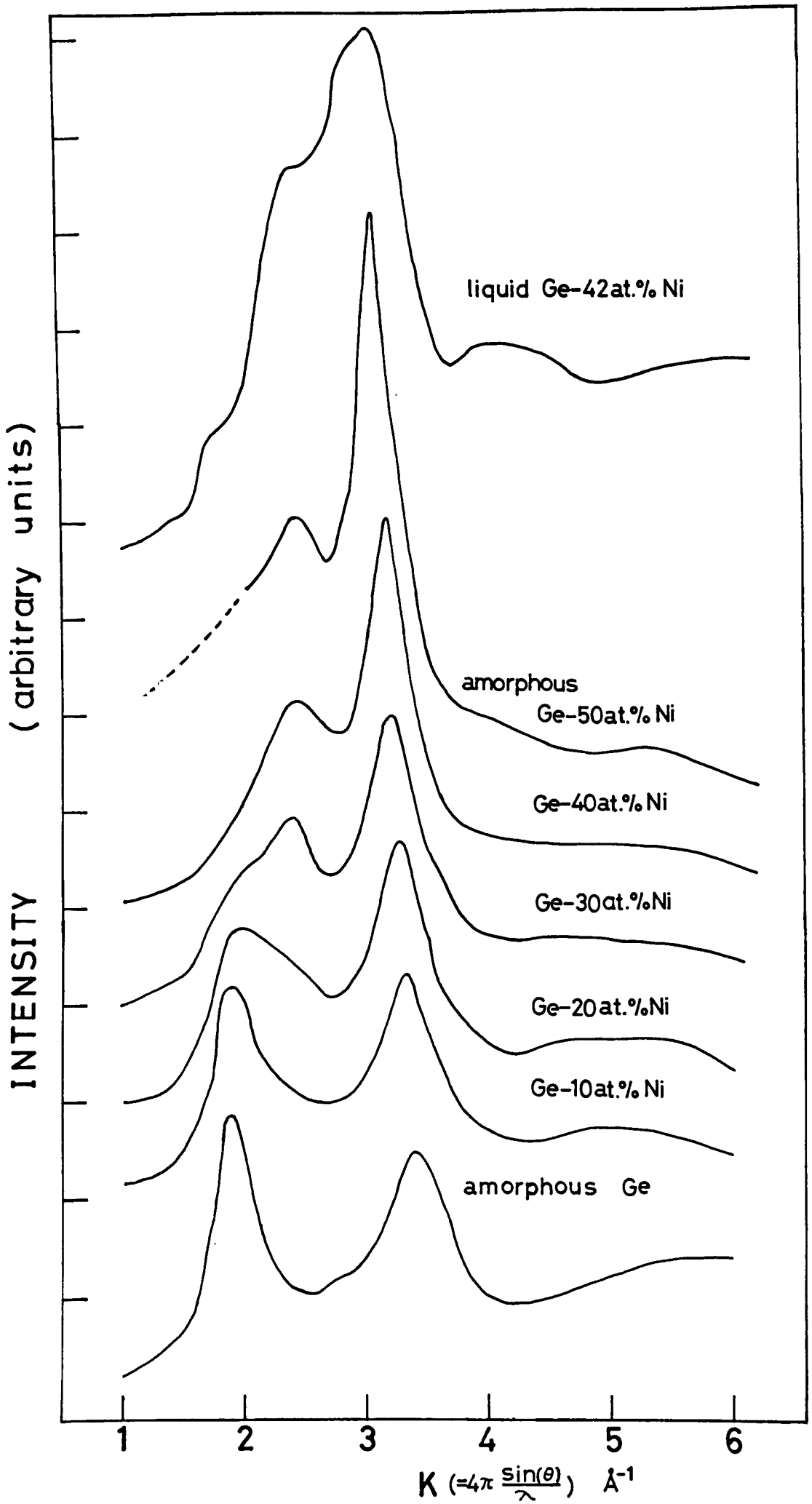
liquid Ge-42at.% Ni
amorphous
Ge-50at.% Ni
Ge-40at.% Ni
Ge-30at.% Ni
Ge-20at.% Ni
Ge-10at.% Ni
amorphous Ge
INTENSITY (arbitrary units)
1
2
3
4
5
6
K (=4π sin(θ)/λ) Å-1

Fig. 2

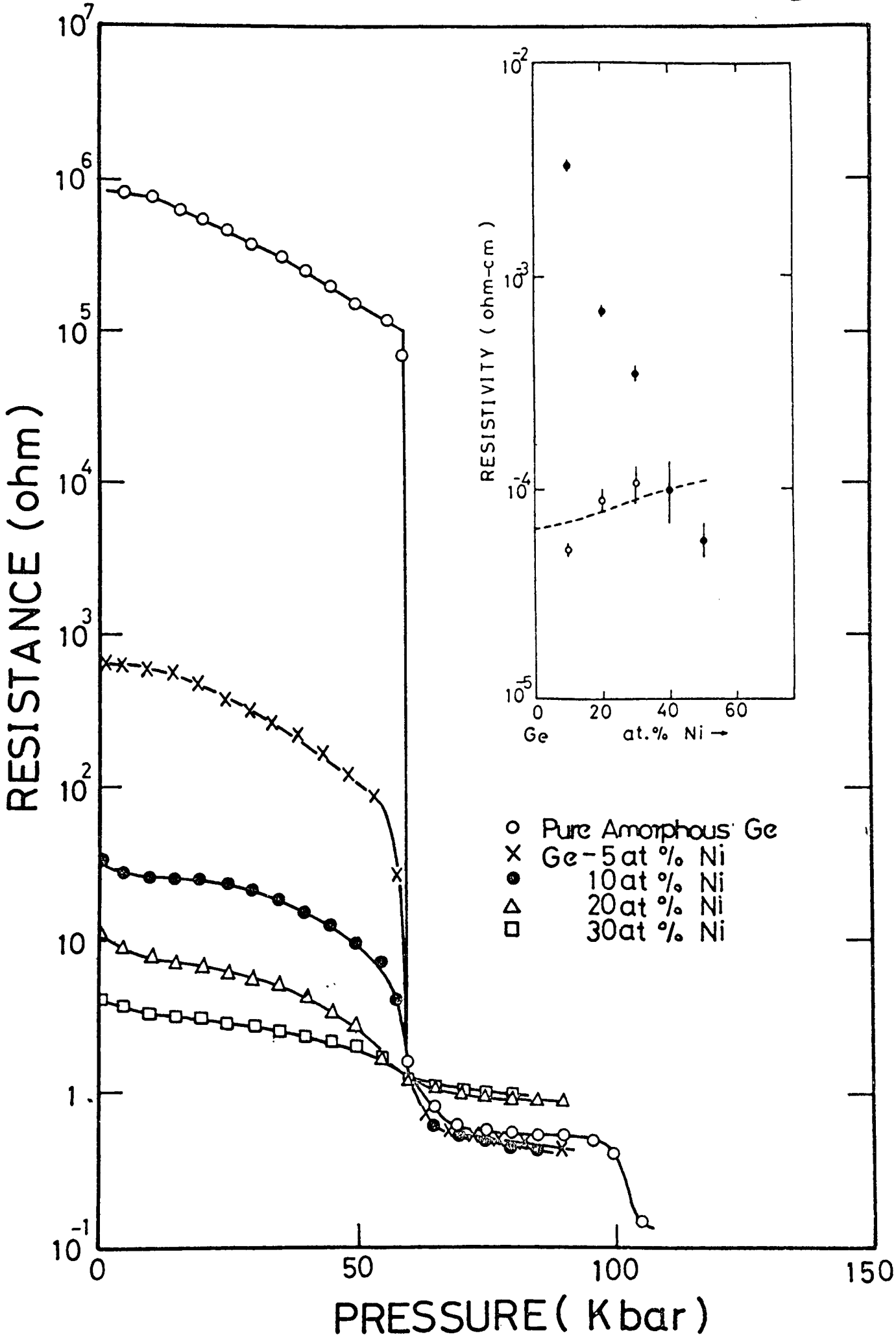
RESISTANCE (ohm)
PRESSURE (Kbar)
RESISTIVITY (ohm-cm)
at.% Ni →
Ge
Pure Amorphous Ge
Ge-5at % Ni
10at % Ni
20at % Ni
30at % Ni

Fig. 3

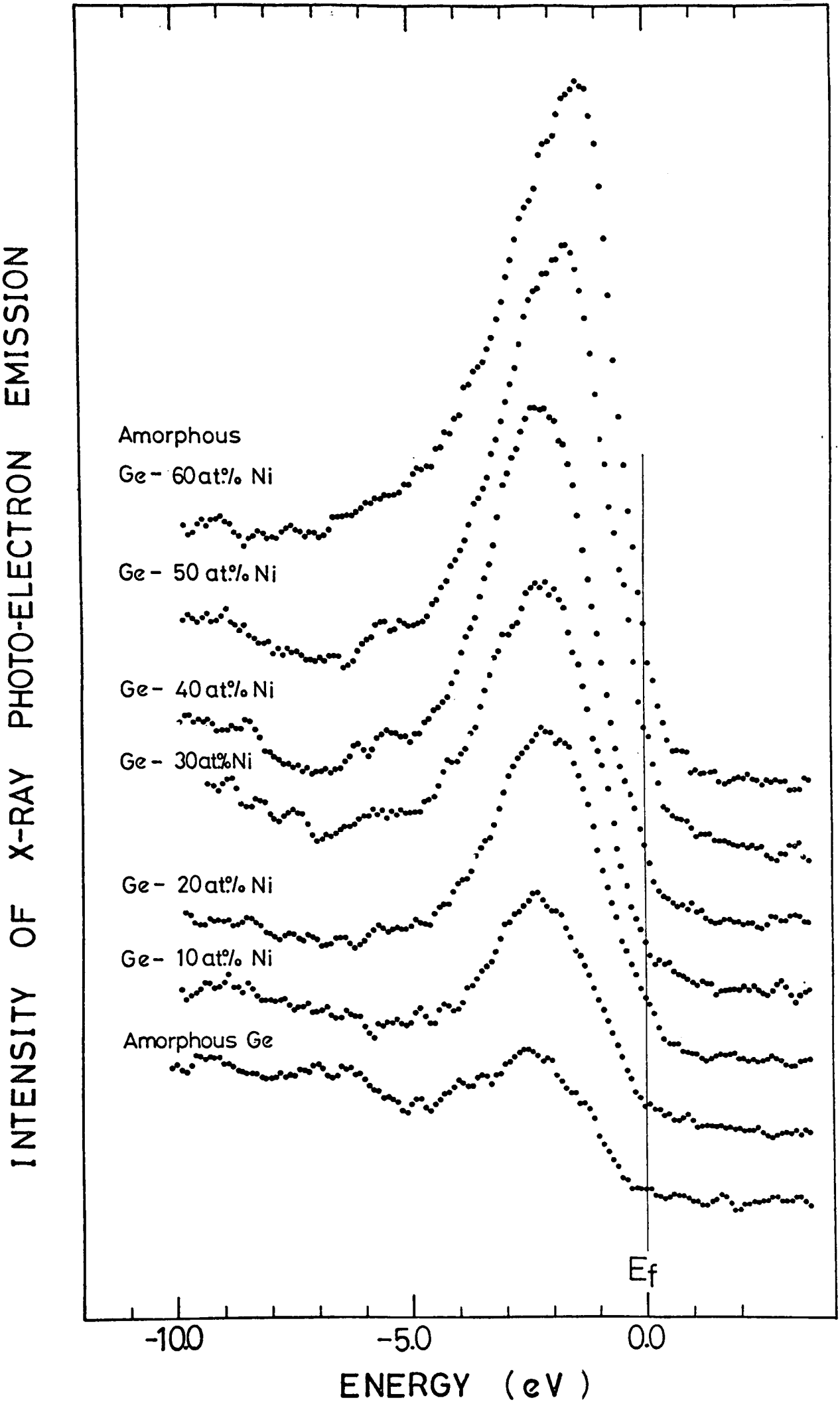
INTENSITY OF X-RAY PHOTO-ELECTRON EMISSION
Amorphous
Ge - 60 at% Ni
Ge - 50 at% Ni
Ge - 40 at% Ni
Ge - 30 at% Ni
Ge - 20 at% Ni
Ge - 10 at% Ni
Amorphous Ge
Ef
-10.0
-5.0
0.0
ENERGY (eV)

Fig. 4

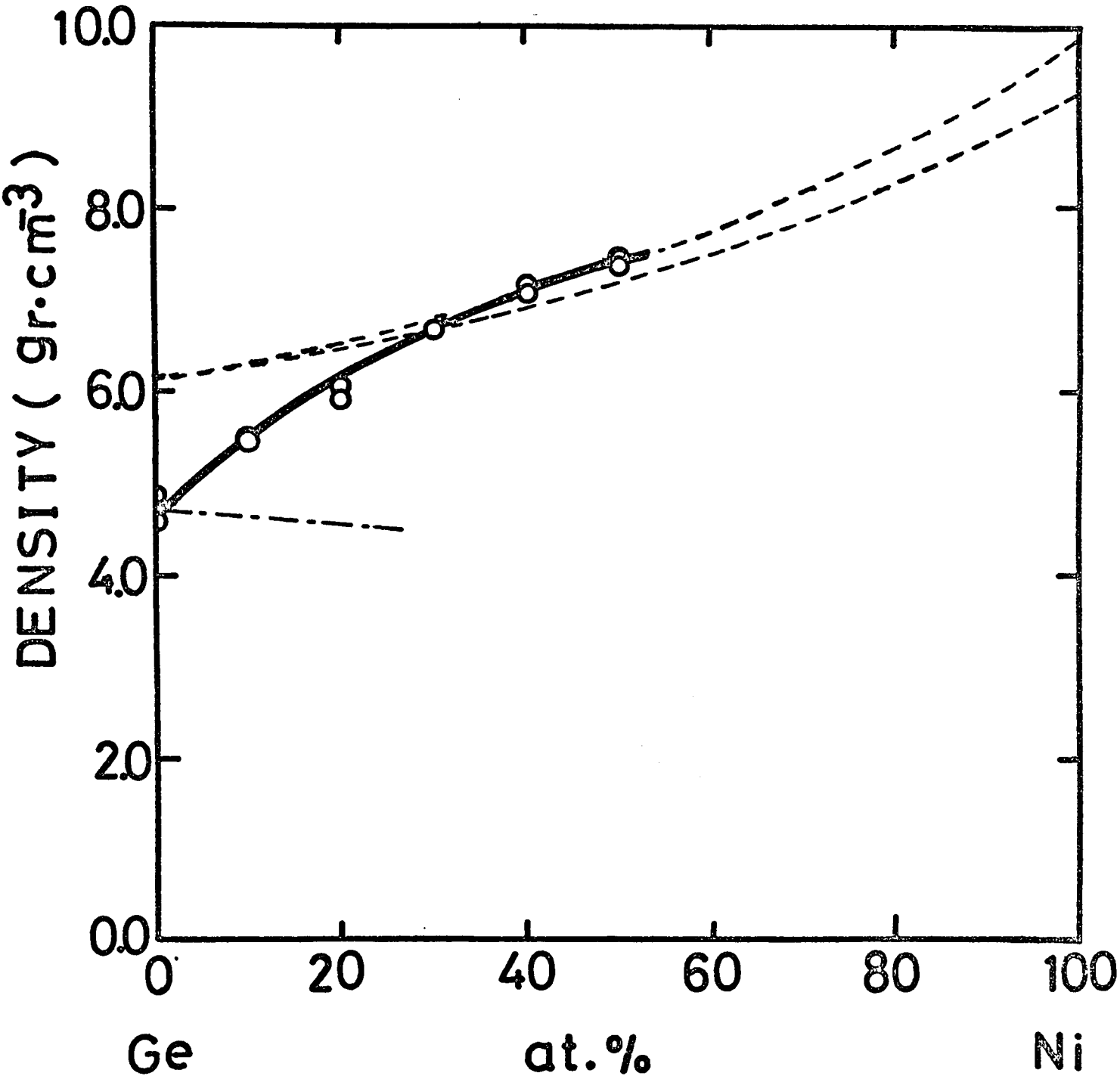

Part III

X-ray Photoemission Spectra of Valence Bands in Amorphous Ge-Ni, Ge-Fe and Ge-Au Alloys

§1 Introduction

Most metals are free to dissolve in one another when they are liquid, and the atomic and electronic structure of number of different alloy systems have been investigated as a function of concentration in the liquid state. However there are very few systems which show a complete range of solution in both the liquid and the solid phase. For Ni-Ge system, the two constituents are only slightly soluble in a Ni rich phase in solid state and form so-called electron compounds which exist as Ni_3 Ge with the structure of Cu_3Au type and NiGe with the structure of MnP type. For Fe-Ge, the solubility of Fe in Ge is very low and it is also impossible to make crystalline alloys of Ge and Au in a whole concentration range. However the Ni-Ge, Fe-Ge and Au-Ge systems are completely miscible when liquid. The precise measurements for the physical properties of these alloys are not easy, since their melting temperatures are considerably high.

It has been shown that the amorphous alloys of Ge-Ni, Fe and Au with various concentrations can be easily produced by evaporation onto a substrate. The X-ray or electron diffraction patterns of these alloys show highly diffuse diffraction rings.[1] The X-ray scattered intensity curves I(k) for amorphous Ge-Ni alloys in the concentration range over 30 at.% Ni show similar patterns with those for liquid, though there are large differences in the structural and electrical properties between amorphous and liquid Ge.[2][3] Recently Stritzher and Wühl have reported that the amorphous Ge-noble metal alloys obtained by condensation become superconducting in the range of concentration between 25

and 80 at.%Au and Cu.[4] The superconductivity of these phases is believed to be due to Ge forced into a metallic liquid-like structure with a higher coordination number than that of the semiconducting diamond structure. Therefore it is interesting to study the systematic variation of atomic and electronic structure of such amorphous alloys with concentration and also the extent of the similarity of physical properties in these amorphous alloys with those in liquid state.

Bush et al.[5] have measured the electrical resistivity, magnetic susceptibility and Hall coefficient of liquid Ge-Fe, -Co,-Ni and-Cu alloys. The concentration range which shows the negative temperature coefficients for the resistivity of Ge alloys increases from Cu to Fe alloys. From the experimental data for the concentration dependence of the electronic properties of these alloys, they have suggested the following schematic density of states of d-electrons for different concentration of Fe-Ge alloys. For pure liquid Fe, the density of states is split into two peaks and the Fermi energy lies on the low energy side of the high energy peak. On alloying with Ge, the splitting is reduced, the middle of the 3d-band and Fermi energy move into the positions of the virtual bound state for liquid Ge rich alloys. Therefore, the density of states at the Fermi energy increases for Fe rich alloys and decrease beyond a certain concentration, for which the Fermi energy moves through the second, but reduced peak. Therefore it is interesting to obtain the information concerning the density of states for these alloys.

Recently many investigators have carried out the measurement for the density of states of Ni, Co, Fe, Au, and Cu etc. by

using X-ray photoelectron spectroscopy (XPS) technique.[6][7][8] They have shown that XPS can in principle provide a rather direct determination of the density of states near the Fermi level as well as very precise information on core electron binding energies. Since the kinetic energy of the photoemitted electron is very large compared with the band width and the energy losses due to the scattered electrons photoexcited inside the sample are distributed over a large range, the use of XPS technique ensures the predominantly bulk nature of the transition, a small contribution of inelastically scattered electrons, and nearly energy-independent escape depth. Baer and Bush[9] have studied by using XPS technique the density of states of Al which is well known as one of nearly free electron metals and found the striking similarity of the valence band spectrum with computed density of states. This study of Al demonstrates that XPS is a satisfactory technique for studying the density of states and the different processes involved in the XPS have a weak influence on the shape of band spectrum which is closely related to the density of states.

In the present paper X-ray photoelectron emission studies of amorphous alloys between Ge and Ni, Fe and Au are reported X-ray photoelectron emission spectra have been obtained which contain information about the position and shape of d-bands as well as about the position of core levels.

§2 Experimental Procedure

Spectra were measured on a KEC-X 200 electron spectrometer using the characteristic Al $k\alpha_{1,2}$ X-ray (1.486 KeV) radiation. The kinetic energy of photoemitted electrons was analyzed in a hemispherical electrostatic analyzer and the energy selected by the spectrometer was varied in step of 0.1 eV. The counts at each energy were accumulated. The total instrumental resolution including the X-ray line width is slightly better than 1.0 eV.

To prepare amorphous specimens, the mixtures of Ge and Ni, Ge and Fe, and Ge and Au with various concentrations, rapidly quenched from their melts, were evaporated onto clean stainless steel plate at room temperature from the tungsten filament in the sample preparation chamber. The tungsten filament and Ge alloys were carefully outgassed. The background pressure was initially 1×10^{-5} mm Hg and it rose to 2×10^{-5} mm Hg during the evaporation. The sample was carefully evaporated step by step for a very short period to prevent the crystallization of the condensed sample due to the radiation from tungsten filament. The total evaporation time was one minute. The distance between the substrate and tungsten filament was about 10 cm. The thickness of amorphous films obtained by evaporation was about 500 A. The films were then directly transferred to the analyzer. On recording the spectra, the vacuum of photoemission chamber was maintained at 10^{-7} mm Hg.

In spite of this careful preparation, O(1s) and C(1s) were present in the spectra. The intensity ratios of the contaminant O(1s) to Ge(3d), Ni(2p), Fe(2p), and Au(4f) lines were very small

and no increase of the intensity ratio was observed during the measurements. There was no change of the shape in the core level signals due to the oxide formation in Ni, Fe and Au atoms near the surface. All runs were made under the condition which O(1s) line had negligible intensity and the core levels have narrow and stable widths.

Since the evaporation rates of the constituent atoms in alloys might be different, there could be some ambiguities for the determinations of alloy concentrations of the sample. It was seen that the intensities of the inner core levels in the Ni, Fe and Au changed almost linearly with the corresponding concentration.

§3 Experimental Results

The ionic structures of Ge-Ni, Ge-Fe and Ge-Au alloy films used for the present measurements are amorphous, except pure Ni, Fe and Au. For pure Ni, Fe and Au specimens it is impossible to obtain the amorphous states by condensation at room temperature. In the previous paper[1] we reported the X-ray scattered intensity curves of amorphous Ge-Ni alloys. It is well known that there are large differences in the structural and electronic properties between amorphous and liquid Ge. Amorphous Ge behaves like a semiconductor, while liquid Ge like metal. However X-ray patterns of amorphous Ge-Ni alloys remarkably change with increasing concentration of Ni, and become similar to those in liquid alloys in the range of Ni concentration over 30 at.% , where transition from semiconducting to metallic state occurs.

Fig. 1 shows the experimental valence band spectra from amorphous Ge-Ni alloys without any correction. To get the "true" density of states, corrections have to be applied to the data. The transition probabilities are a function of the energy of the initial state, varying by about 10 % over the width of the d-band in Ni. It is at present impossible to correct for this effect. The Fermi energy was determined, with a thin layer of Au evaporated at the position where the 6s-band is down to half its height. The spectrum of the valence band of Ni forms a narrow band as a result of the comparatively localized nature of the d-wave function and appears as a single peak with maximum intensity at -1.0 eV below E_F and a half width of the order of 2.7 eV. The maximum density of states can be

somewhat closer to the Fermi level as a consequence of the total instrumental broadening. The main peak associated with Ni d-states in the density of states of amorphous Ge-Ni alloys shows a remarkable shift to lower energies with respect to the Fermi level E_F with addition of Ge to Ni. In high concentration region over 70 at.% Ge, where alloys show semiconducting property, the change of position of peak is relatively small with increasing concentration of Ge and it is difficult to determine precisely the positions of the peaks since the peaks merge into broad valence band of Ge. The half width of the main peak becomes narrower with increasing concentration of Ge, though there are considerable ambiguities for the estimation of the half-width because of a high background at low energy region.

The raw data for the valence band regions of amorphous Ge-Fe alloys are shown in Fig. 2. The spectrum of the valence band in Fe is broadened towards lower energies because of the high contribution of small energy losses and no precise location of the bottom of the band is possible in this case. The spectrum shows a main peak with maximum at -1.2 eV. The main peak in the density of states associated with Fe d-states shifts towards lower energies relative to E_F with addition of Ge to Fe. The change of positions of the main peaks in the spectra of amorphous Ge-Fe alloys is comparatively small in the Ge rich range of concentration nearly as same as in the case of amorphous Ge-Ni alloys. The half width of main peak decreases with increasing of Ge content.

Fig. 3 shows the valence band spectra from amorphous Ge-Au

alloys. The photoelectric cross section of Au is extremely high compared to the other metals. The peaks originated from the d-state of Au sites appear in the spectrum when only 2 at.% Au is added to Ge. The intensities of the spectra shown in Fig. 3 are normalized for the heights of the maximum peaks to be the same for the all of spectra. The half width of the d-band of pure Au is approximately 5.4 eV and the two separated peaks are located at -3.2 eV and -6.0 eV. The contribution of scattered electrons to the spectrum is very small and has a negligible influence on the band shape. The position of the peak which lie at lower energy side does not change on alloying with Ge, while that at higher energy side remarkably shifts towards lower energies relative to E_F.

Fig. 4, 5 and 6 show the positions of peaks with respect to E_F in Ge $3d_{3/2}$ core electron spectra obtained from the measurement for Ge-Ni, Fe and Au alloys. The positions with respect to E_F are almost independent of the concentration of alloys within the experimental errors.

The positions of Ni $2P_{3/2}$ core level with respect to E_F in Ge-Ni alloys are plotted as a function of concentration in Fig. 7. The position of Ni $2P_{3/2}$ core level with respect to E_F shifts to lower energies with increasing Ge. As shown in Fig. 8, only small shifts of Fe $2P_{3/2}$ core level are observed for Ge-Fe alloys. Fig. 9 shows the concentration dependences of Au $4f_{7/2}$ and $4f_{5/2}$ core levels with respect to E_F in Ge-Au alloys. The change of Au $4f_{7/2}$ core level is quite similar to that of Au $4f_{5/2}$. The positions of Au $4f_{5/2}$ and $4f_{7/2}$ core levels are found to undergo considerable changes with Ge concentration, and the positions shift to lower energies with the addition of Ge, as in the case

of Ge-Ni alloys.

§4 Discussion

The physical properties of the transition metal alloys were first discussed by Mott[10] on the basis of a rigid band model. This model assumes that the parent metals and alloys of them have the same distribution of energy states, and these states are filled to a level appropriate to the electron-to-atom ratio of the system. Cu-Ni alloy which has long been considered the prototype alloy whose magnetic properties are explained by the rigid band model. However the recent measurements of X-ray photoelectron emission by Hufner et al.[11] has demonstrated that rigid band model is quite inappropriate for all Cu-Ni alloys. In alloys of Cu-Ni, Cu d-states are located in the energy region associated with Cu d-states in pure Cu and similarly Ni d-states are located in the energy region associated with Ni d-states in pure Ni. The density of states of Cu-Ni alloys can be made up by superimposing those of Ni and Cu. Therefore there is indeed only a very limited sharing of electrons by the two constituents. The density of states of Cu-Ni alloys at the Fermi level deduced from their data is in good agreement with theoretical predictions based on the coherent potential approximation.[12]

Takekura and Kanamori[13] have discussed the electronic structure of impurity atoms of non-transition elements in transition metal (Al in Ni and Pd, etc.) on the basis of ab initio calculation with the use of pseudo-Greenian method.[14] The valence orbitals of s and p symmetries of the impurity atom may combine with the s, p and d orbitals of surrounding host atoms to form bonding and antibounding molecular orbitals. According to their calculation, the density of states for the s or p orbitals

of Al as impurity in Ni shows generally a hump below or in the lower half of the d-bands; it is followed then by a dip which is broad for the s-orbital extending in the whole range of the d-bands. For the p-orbitals, the bottom of the dip is situated around the top of the d-bands.

The variations of the positions of main peaks associated with the d-states of Ni and Fe with concentration are plotted in Fig. 10. The main peaks associated with d-states of Ni and Fe in the density of states of amorphous Ge-Ni and Ge-Fe alloys show the remarkable shift to lower energies with respect to the Fermi level with addition of Ge to Ni and Fe.

The valence orbitals of Ge may combine with the s, p, and d orbitals of surrounding Ni atoms to form bonding and antibonding orbitals. As a result, the density of states of Ge in Ni may have a hump with high density distribution of electrons near the bottom of the d-band of Ni to form bonding state. Therefore the shift of main peak to lower energies with addition of Ge as shown in Fig. 10 may suggest that the valence orbitals of Ge combine with the d-orbital of Ni to form bonding orbitals, and this bonding states extend with increasing Ge content, eventually to that of valence orbitals of Ge. It is interesting that in the high concentration region over 70 at.% Ge, where alloys show semiconducting property, the change of position of peak is relatively small with increasing concentration of Ge.

The same explanation for the shift of main peak above mentioned may be also appropriate to the case of Ge-Fe alloys.

The positions of main peaks of d-states of Au are situated in the low energies, much lower than those of Ni and Fe. In the

photoelectron emission spectra of Au-Ge alloys the middle of main peak associated with d-states of Au moves towards lower energies referred to E_f. It is noticed that the main peaks do not continuously merge into the valence band structure of Ge with decreasing concentration of Au in contrast to the cases of Ni-Ge and Fe-Ge alloys.

The splitting of the peak associated with the d-band of Au observed for Au-Ge alloys is believed to be a spin orbit effect. Fig. 12 shows the variation of the separation between two peaks with Ge concentration. The separation between peaks decreases with increasing Ge content in the alloys. This evidence may be attributed to the mixing of the d-orbital in Au with the s, p-orbitals in Ge.

The apparent variation of Ni $2P_{3/2}$, Fe $2P_{3/2}$, and probably of Au $4f_{5/2}$ and $4f_{7/2}$ core levels with alloying may be attributed to the change of Fermi level since Ni $2P_{3/2}$ and Fe $2P_{3/2}$ core levels lie in considerably lower energies with respect to Fermi energy. Thus, as shown in Fig. 12, it is reasonable assumption that the Fermi levels of Ge-Ni, Ge-Fe and Ge-Au shift towards to higher energies with the addition of Ge to Ni, Fe and Au. It is noticed that the change of the Fermi level in Ge-Fe with Ge concentration is quite small compared to other alloys. Fig. 13 shows that the $3d_{3/2}$ core levels of Ge in Ge-Ni, Ge-Fe and Ge-Au alloys are shifted towards lower energies by the same amounts corresponding to a highering of the Fermi level. Therefore, the electron binding energies of core levels of Ge in Ni, Fe and Au are higher compared to that in pure Ge and decrease with increasing of Ge concentration.

The fact that the electron binding energy of $3d_{3/2}$ core level of Ge in Ni is higher compared with that in pure Ge as shown in Fig. 13 suggests the transfer of charge from Ge atoms to Ni atoms to form the bonding between Ge and Ni. The charge flow due to the bonding between Ge and Ni decreases with increasing Ge concentration.

The measurement of the Mössbauer isomer shift for Au alloys[15] indicates that there is a rather substantial flow of s-like electron charge onto Au sites on alloying, consistent with the view that Au is relatively electronegative. This evidence is entirely consistent with the behaviour observed for Ge-Au alloys in the present work.

Our spectra for the pure amorphous Ge is in excellent agreement with the recent results obtained by Ley et al.[16] The density of states of the valence band of amorphous Ge extends 15 eV below E_F. As pointed out by Ley et al., the gross variation of intensity for the amorphous Ge with respect to energy is similar to the crystalline Ge measured by them. The peak near E_F arised from p-like bonding orbital remains essentially the shape of crystalline Ge and other two s-like peaks situated in lower energies side observed in crystal merge into a single broad peak of intermediate energy in the amorphous state.

Finally, the photoelectron emission spectra obtained from the present experiment is to be helpful for obtaining the knowledge of the density of states in liquid alloys.

It may be considered that the spectra from the valence bands for amorphous Ge-Ni, Ge-Fe and Ge-Au alloys in the metallic region are similar to those for liquid states.

References

(1) K. Tamura, J. Fukushima, H. Endo, S. Minomura, O. Shimomura, and K. Asaumi; Proc. of 2nd International Conference of the Properties of Liquid Metals, Tokyo, 1972, p. 301 (Taylor and Francis).

(2) G.A.N. Connel and W. Paul, J. Non-crystalline Solid 8-10 ('72) 215

(3) A. H. Clark, Phys. Rev. 154 ('67) 750

(4) B. Stritzher and H. Wuhl, Proc. of 12th Low Temperature Physics Conference, Kyoto, 1971, p. 339

(5) G. Bush, H-J. Guntherodt, H. U. Kunzi, H. A. Meier, A. ten Bosch and A. Zimmermann; Proc. of 2nd International Conference of the Properties of Liquid Metals. Tokyo, 1972, p. 263, p. 277 (Taylor and Francis)

(6) C. S. Fadley and D. A. Shirley; Phys. Rev. Letters 21 ('68) 980

(7) M. F. Sorokina, O. I. Kljushnikov, S. A. Nemnonov, V. A. Trapeznikov and V. G. Zyryanov; Physica Scripta 4 ('71) 195

(8) Y. Baer, P. F. Heden, J. Hedman, M. Klasson, C. Nordling and K. Siegbahn; Physica Scripta 1 ('70) 55

(9) Y. Baer and G. Bush; Phys. Letters 30 ('73) 280

(10) N. F. Mott, Adv. in Phys. 13 ('64) 325

(11) S. Hufner, G. K. Wertheim, R. L. Cohen and J. H. Wernick; Phys. Rev. Letters 28 ('72) 488

(12) G. M. Stocks, R. W. Williams, and J. S. Faulkner, Phys. Rev. Letters 26 ('71) 253 and Phys. Rev. B4 ('71) 4390

(13) K. Terakura and J. Kanamori, Prog. Theor. Phys. 46 ('71) 1007

(14) J. Kanamori, K. Terakura, and K. Yamada, Prog. Theor. Phys. 41 ('69) 1426 and Prog. Theor. Phys. Suppl. No. 46 ('70) 221

(15) R. L. Cohen, Y. Yafet and K. W. West, Phys. Rev. B3 ('71) 2872

(16) L. Ley, S. Kowalczyk, R. Pollak and D. A. Shirley; Phys. Rev. Letters 29 ('72) 1088

Figure Captions

Fig. 1 XPS valence band spectra for amorphous Ge-Ni alloys. The Fermi energy was determined, with a Au sample, as the position where the 6s band is down to half its height.

Fig. 2 XPS valence band spectra for amorphous Ge-Fe alloys.

Fig. 3 XPS valence band spectra for amorphous Ge-Au alloys.

Fig. 4 Position of Ge $3d_{3/2}$ core electron level with respect to E_f in amorphous Ge-Ni alloys.

Fig. 5 Position of Ge $3d_{3/2}$ core electron level with respect to E_f in amorphous Ge-Fe alloys.

Fig. 6 Position of Ge $3d_{3/2}$ core electron level with respect to E_f in amorphous Ge-Au alloys.

Fig. 7 Change with alloying of Ni $2P_{3/2}$ level with respect to E_f in Ge-Ni alloys.

Fig. 8 Change with alloying of the position of Fe $2P_{3/2}$ level with respect to E_f in Ge-Fe alloys.

Fig. 9 Changes with alloying of the positions of Au $4f_{5/2}$ and $4f_{7/2}$ levels with respect to E_f in Ge-Au alloys.

Fig. 10 Position of the peak associated with d-states referred to E_f in the XPS valence-band spectra of amorphous Ge-Ni and Ge-Fe alloys.

Fig. 11 Shift of Fermi level in amorphous Ge-Ni, Fe, Au alloys.

Fig. 12 Concentration dependence of the splitting of the valence band in Ge-Au alloys.

Fig. 13 Change with alloying of electron binding energies of core levels of Ge in Ni, Fe and Au.

Fig 1

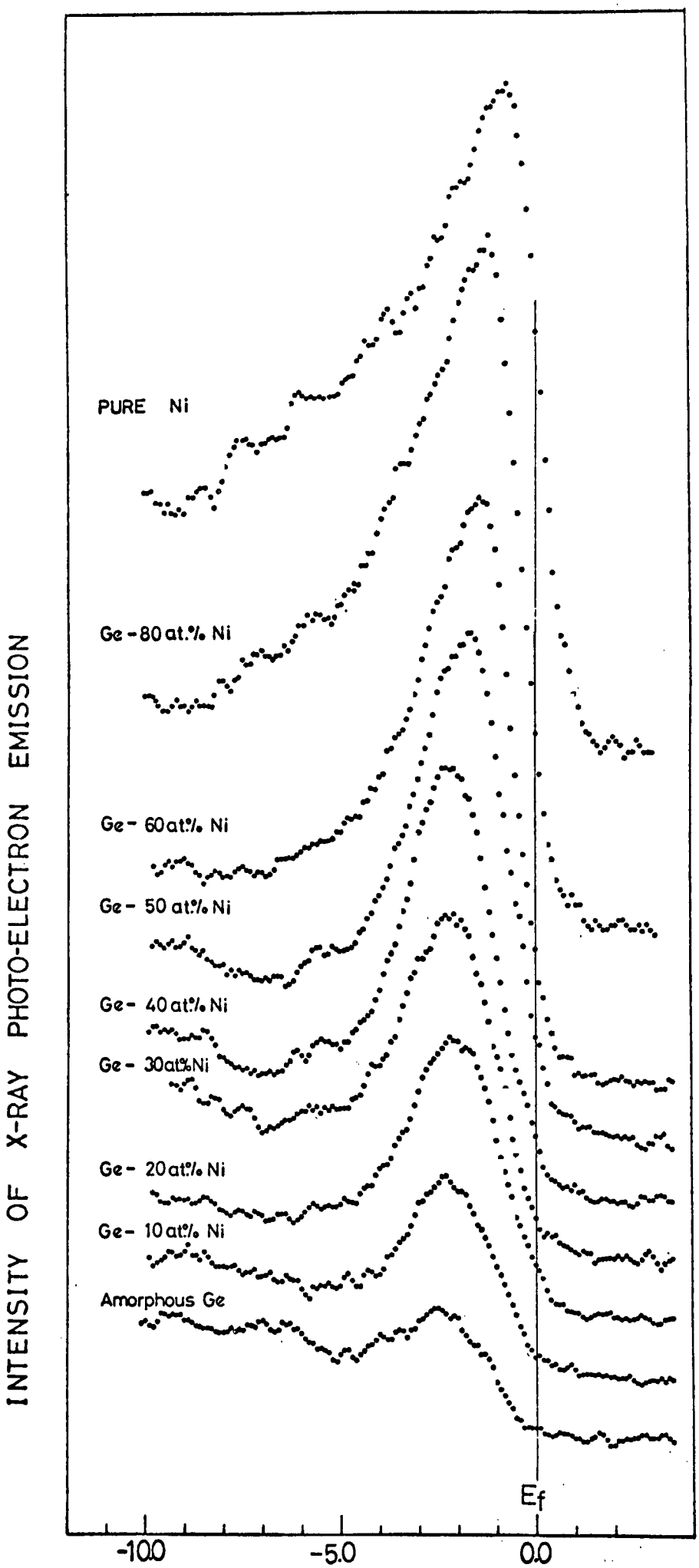
PURE Ni
Ge - 80 at.% Ni
Ge - 60 at.% Ni
Ge - 50 at.% Ni
Ge - 40 at.% Ni
Ge - 30 at.% Ni
Ge - 20 at.% Ni
Ge - 10 at.% Ni
Amorphous Ge
Ef
-10.0
-5.0
0.0
ENERGY (eV)
INTENSITY OF X-RAY PHOTO-ELECTRON EMISSION

Fig. 2

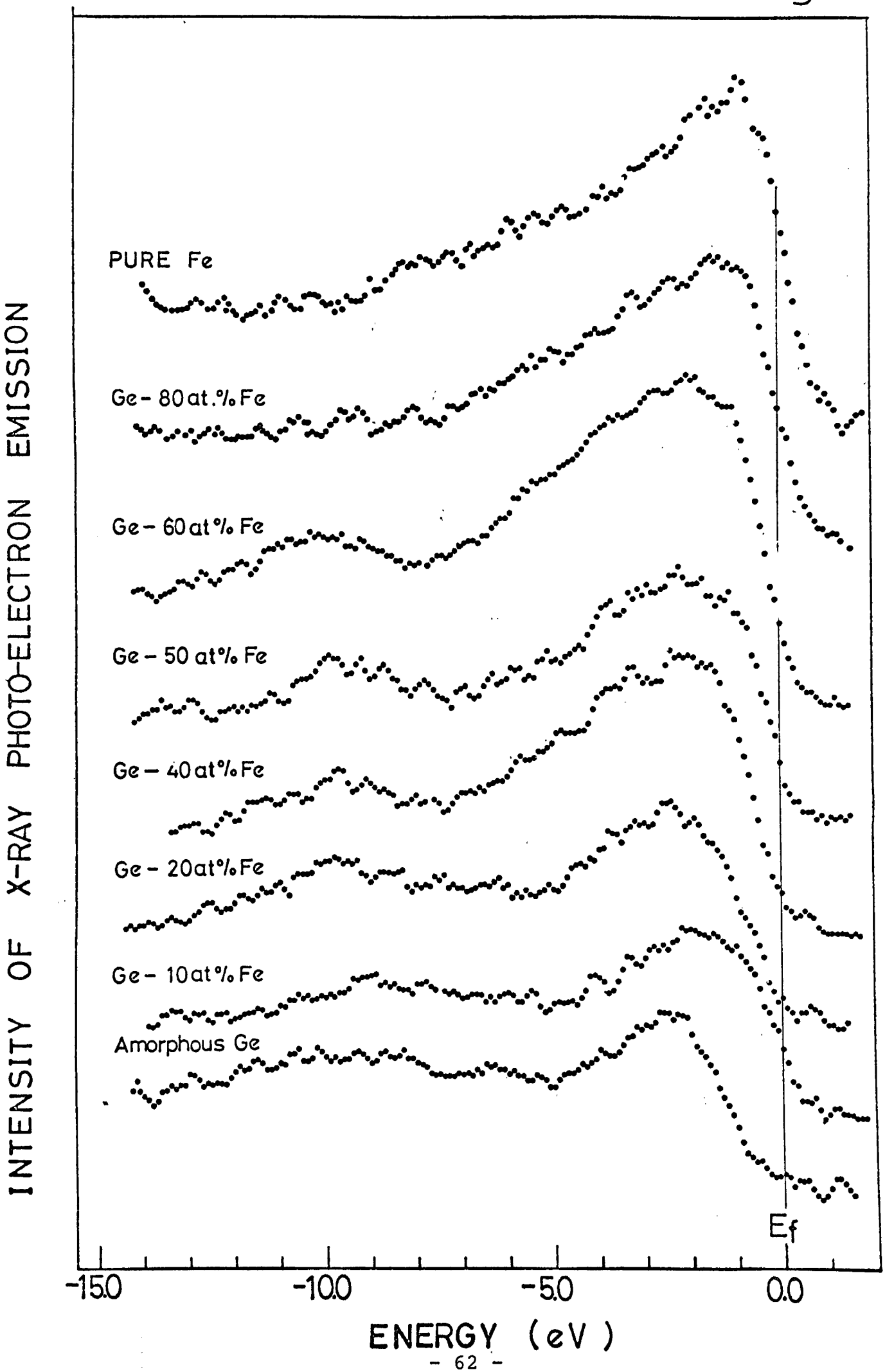
PURE Fe
Ge - 80 at.% Fe
Ge - 60 at % Fe
Ge - 50 at% Fe
Ge - 40 at% Fe
Ge - 20at% Fe
Ge - 10at % Fe
Amorphous Ge
Ef
-15.0
-10.0
-5.0
0.0
ENERGY (eV)
INTENSITY OF X-RAY PHOTO-ELECTRON EMISSION

Fig 3

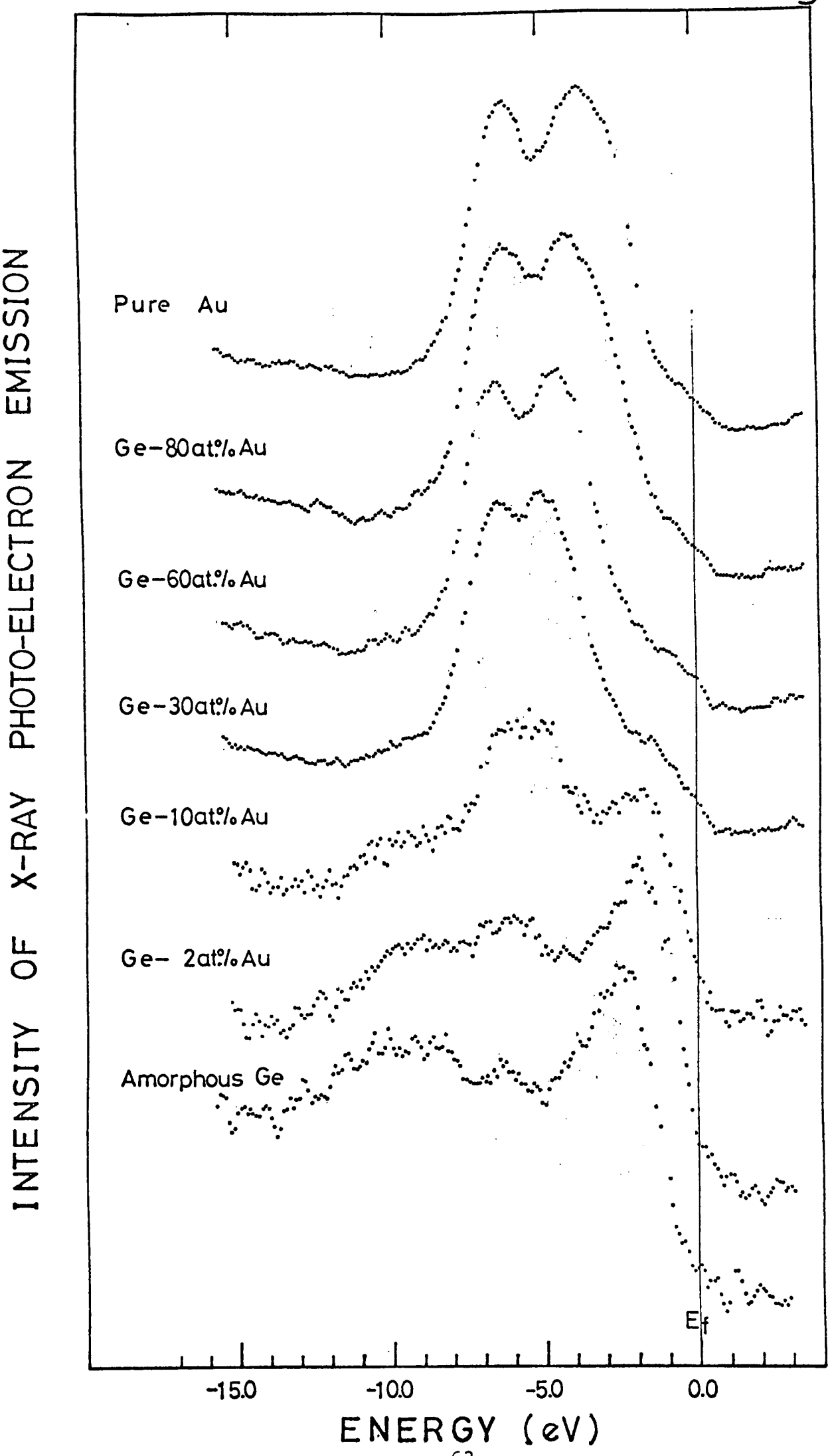
INTENSITY OF X-RAY PHOTO-ELECTRON EMISSION
Pure Au
Ge-80at.% Au
Ge-60at.% Au
Ge-30at.% Au
Ge-10at.% Au
Ge- 2at.% Au
Amorphous Ge
Ef
-15.0
-10.0
-5.0
0.0
ENERGY (eV)

Fig 4

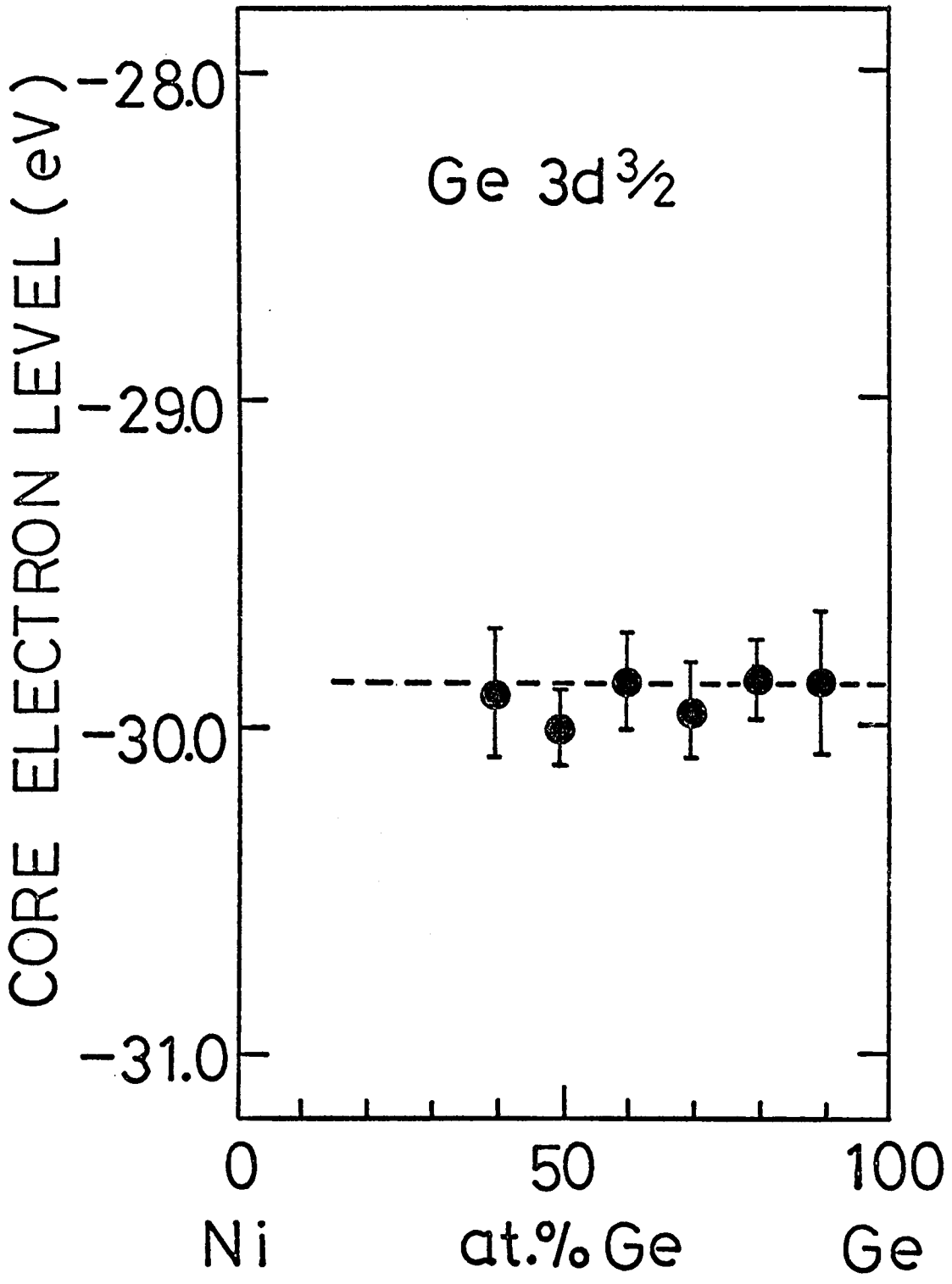
CORE ELECTRON LEVEL (eV)
-28.0
-29.0
-30.0
-31.0
Ge 3d 3/2
0
50
100
Ni
at.% Ge
Ge

Fig 5

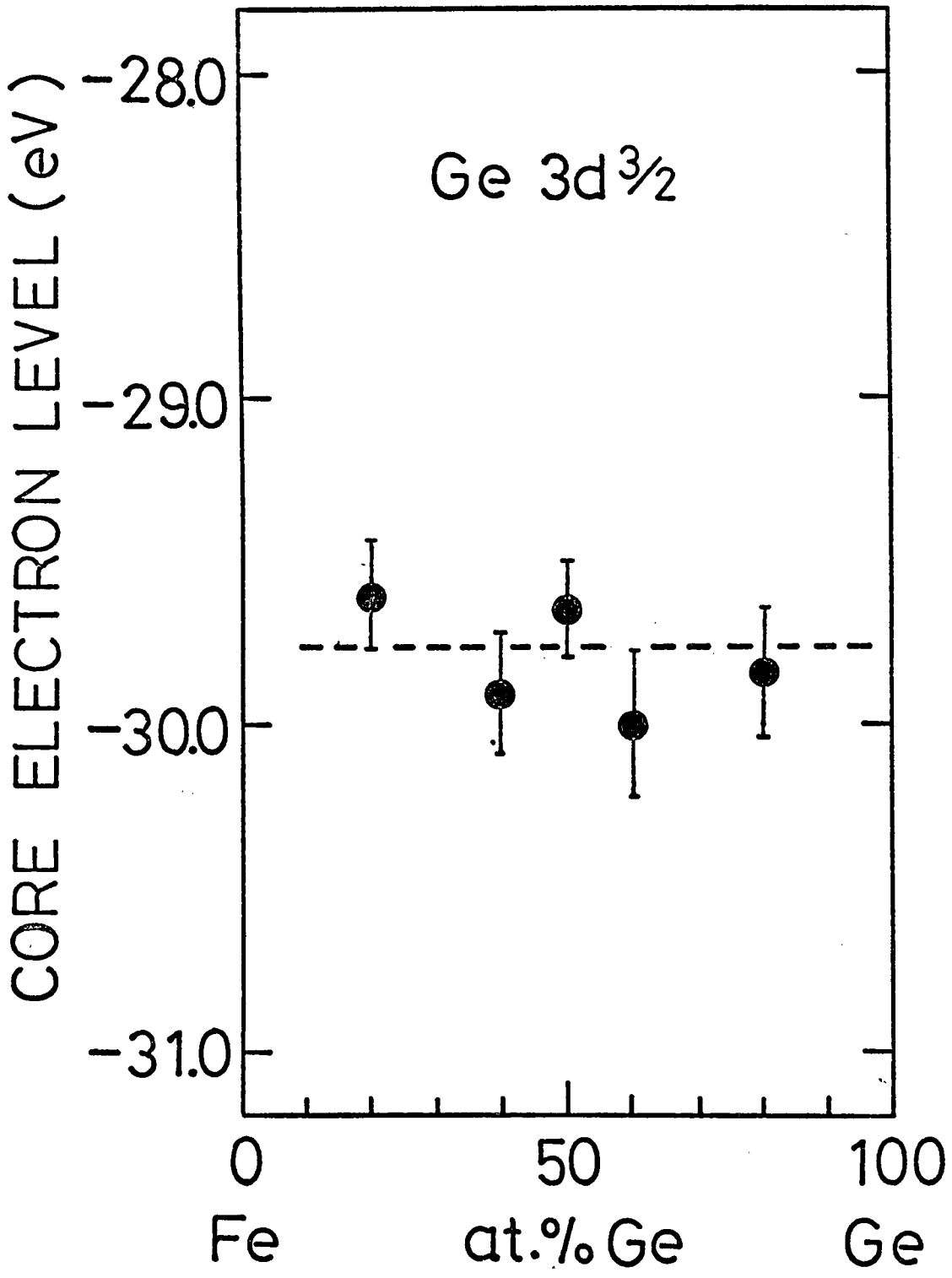
CORE ELECTRON LEVEL (eV)
-28.0
-29.0
-30.0
-31.0
Ge 3d 3/2
0
50
100
Fe
at.% Ge
Ge

Fig. 6

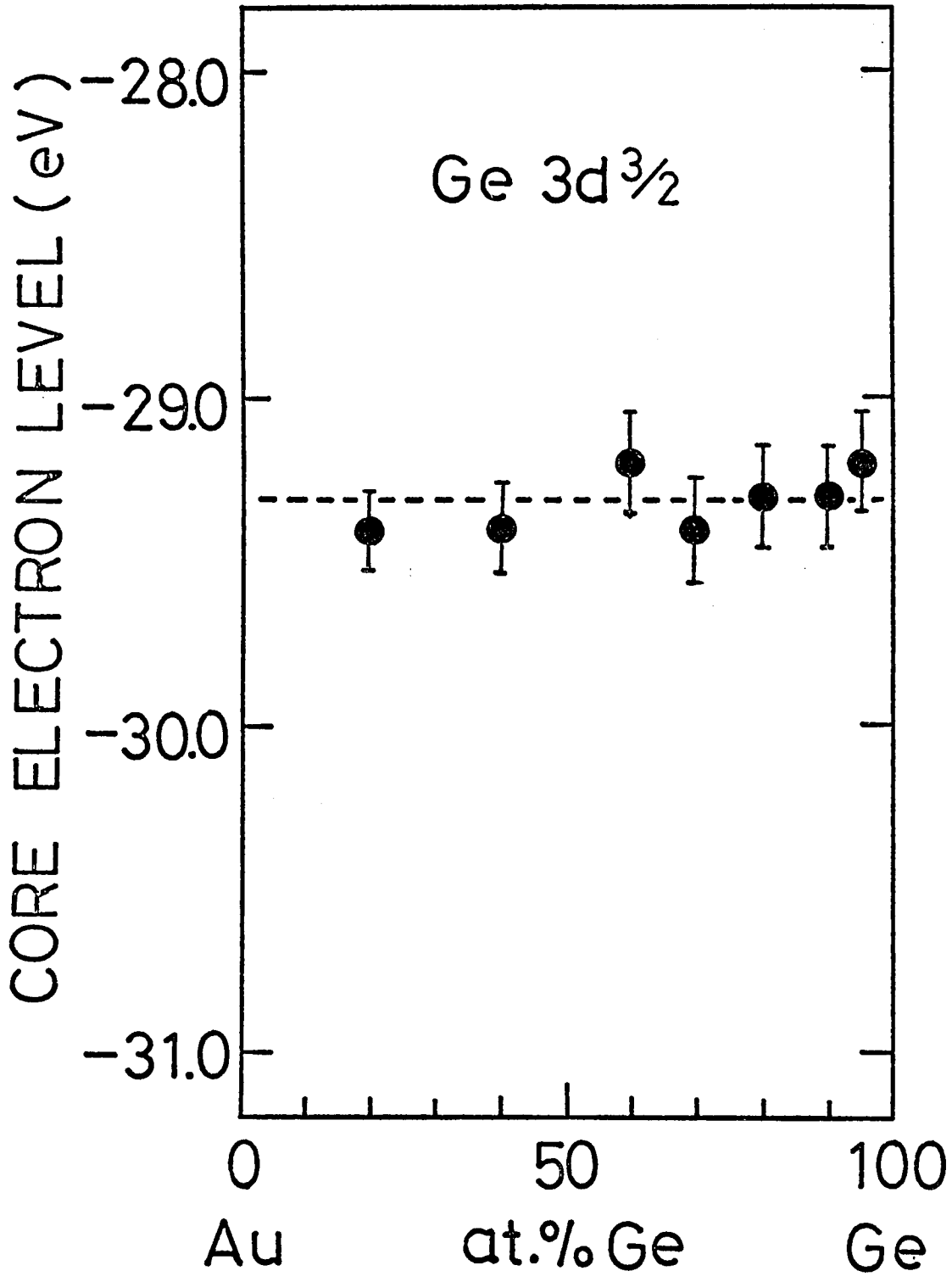
CORE ELECTRON LEVEL (eV)
-28.0
-29.0
-30.0
-31.0
Ge 3d 3/2
0
50
100
Au
at.% Ge
Ge

Fig 7

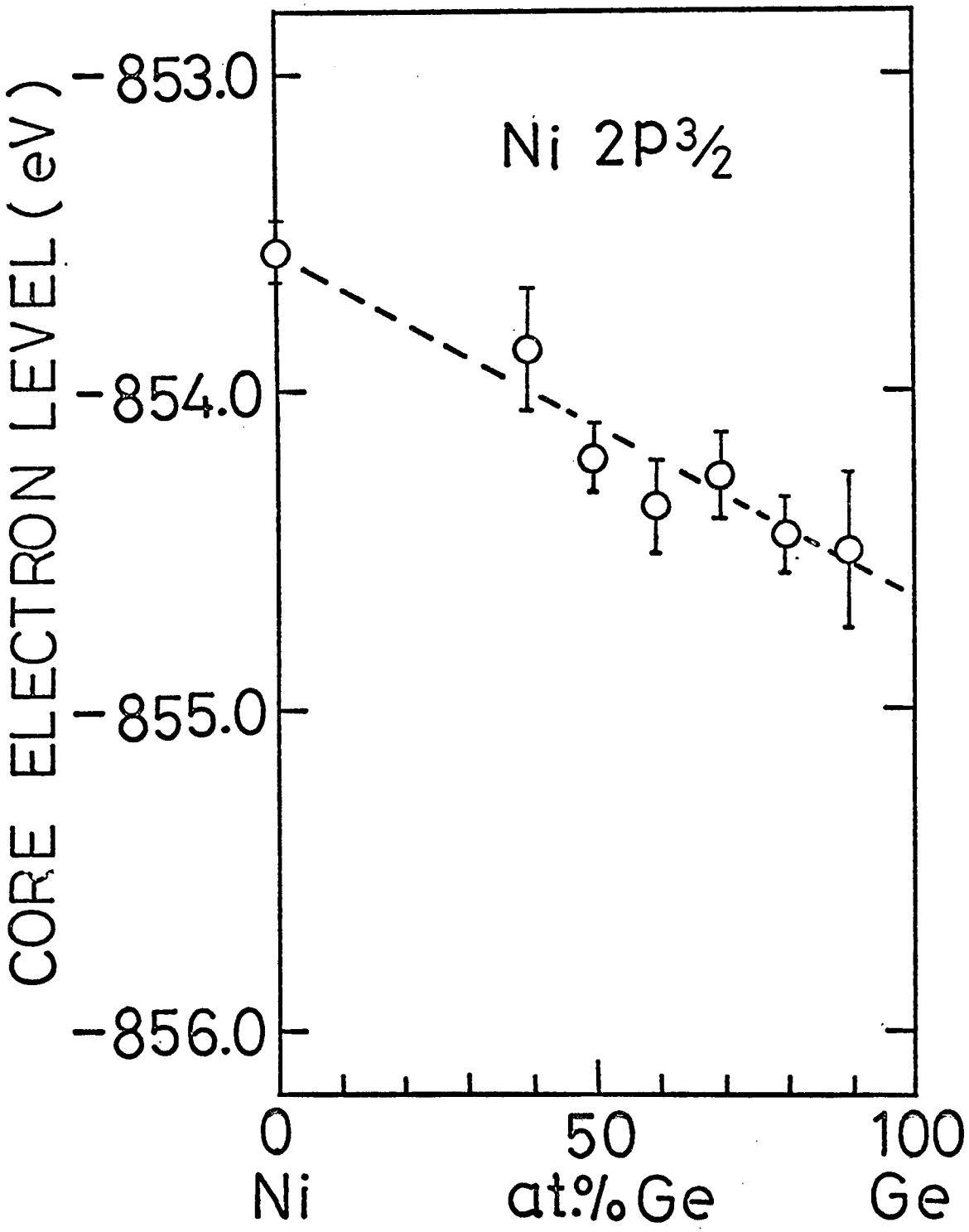
CORE ELECTRON LEVEL (eV)
-853.0
-854.0
-855.0
-856.0
Ni 2P3/2
0
50
100
Ni
at.% Ge
Ge

Fig 8

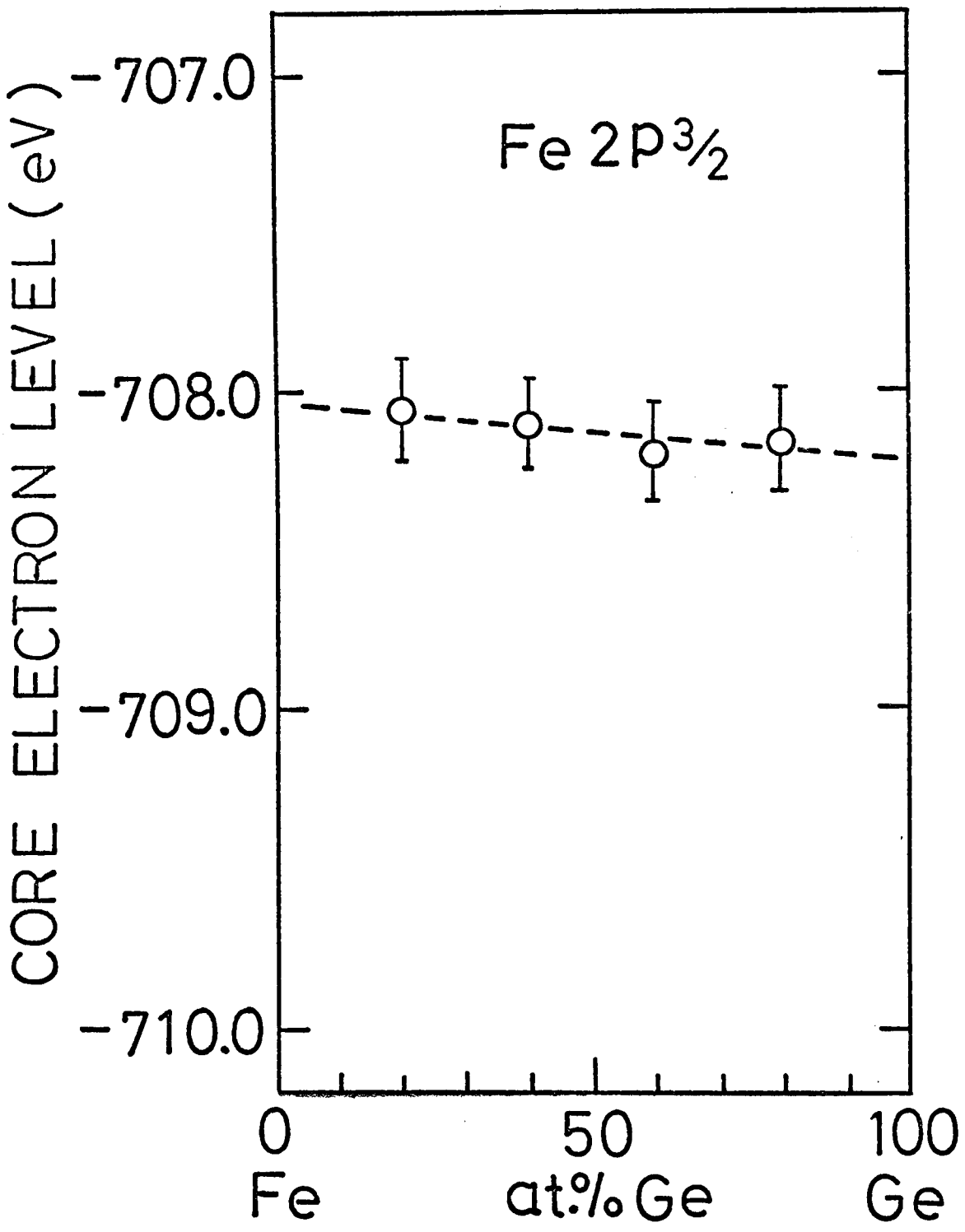
CORE ELECTRON LEVEL (eV)
-707.0
-708.0
-709.0
-710.0
Fe 2p3/2
0
50
100
Fe
at.% Ge
Ge

Fig. 9

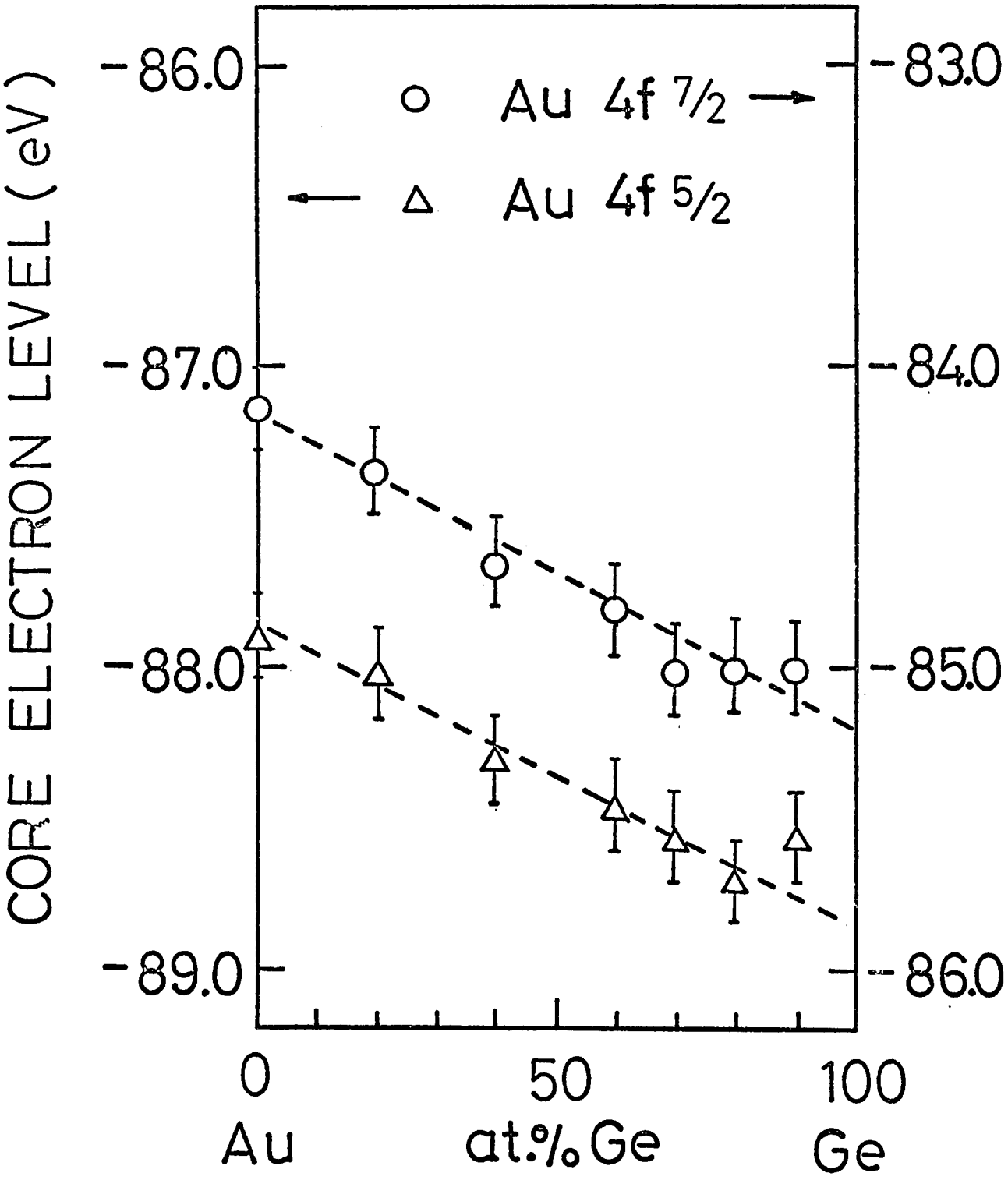
CORE ELECTRON LEVEL (eV)
-86.0
-87.0
-88.0
-89.0
-83.0
-84.0
-85.0
-86.0
Au 4f 7/2
Au 4f 5/2
0
50
100
Au
at.% Ge
Ge

Fig 10

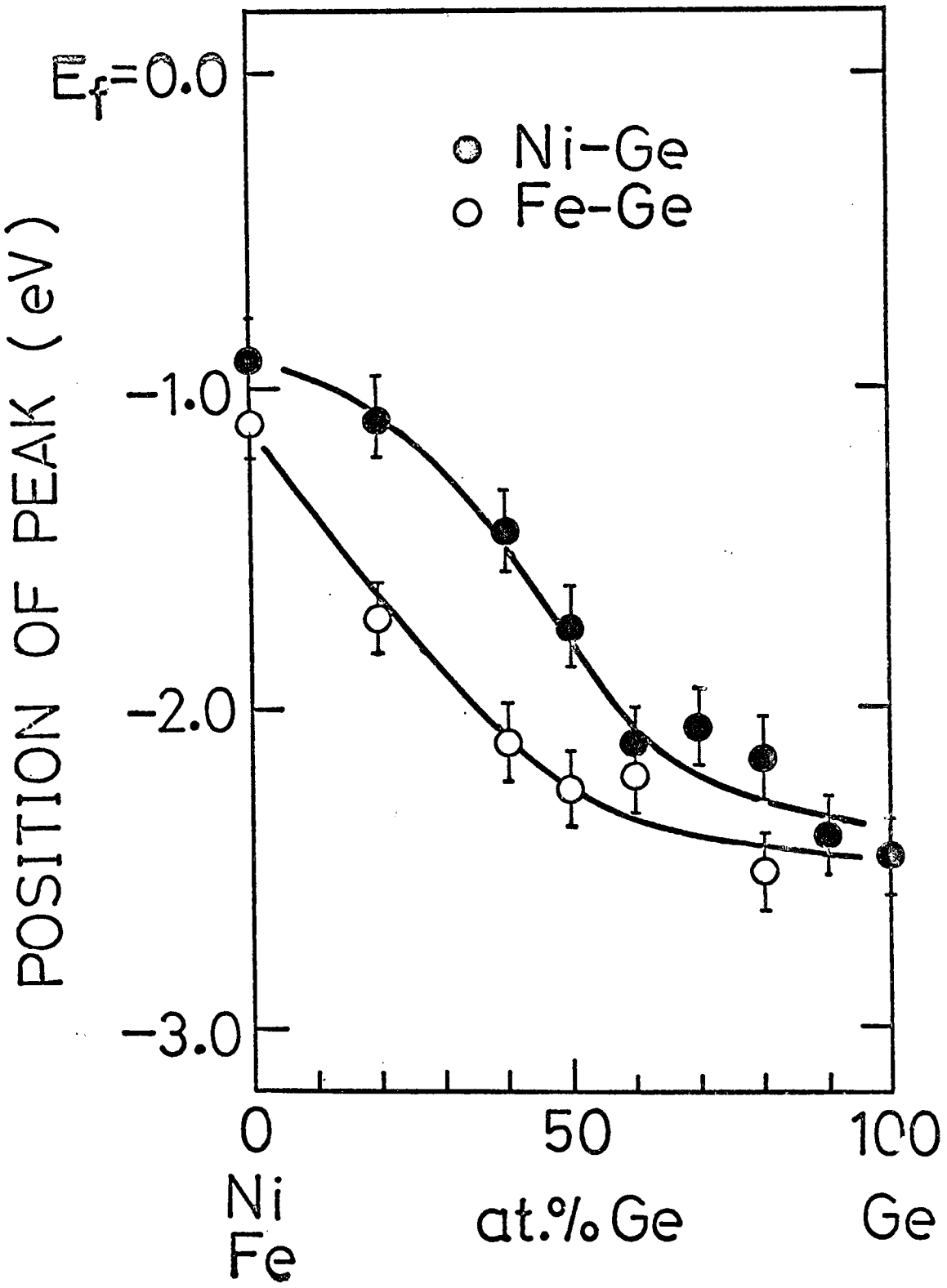
E_f=0.0
Ni-Ge
Fe-Ge
POSITION OF PEAK (eV)
-1.0
-2.0
-3.0
0
50
100
Ni
Fe
at.% Ge
Ge

Fig 11

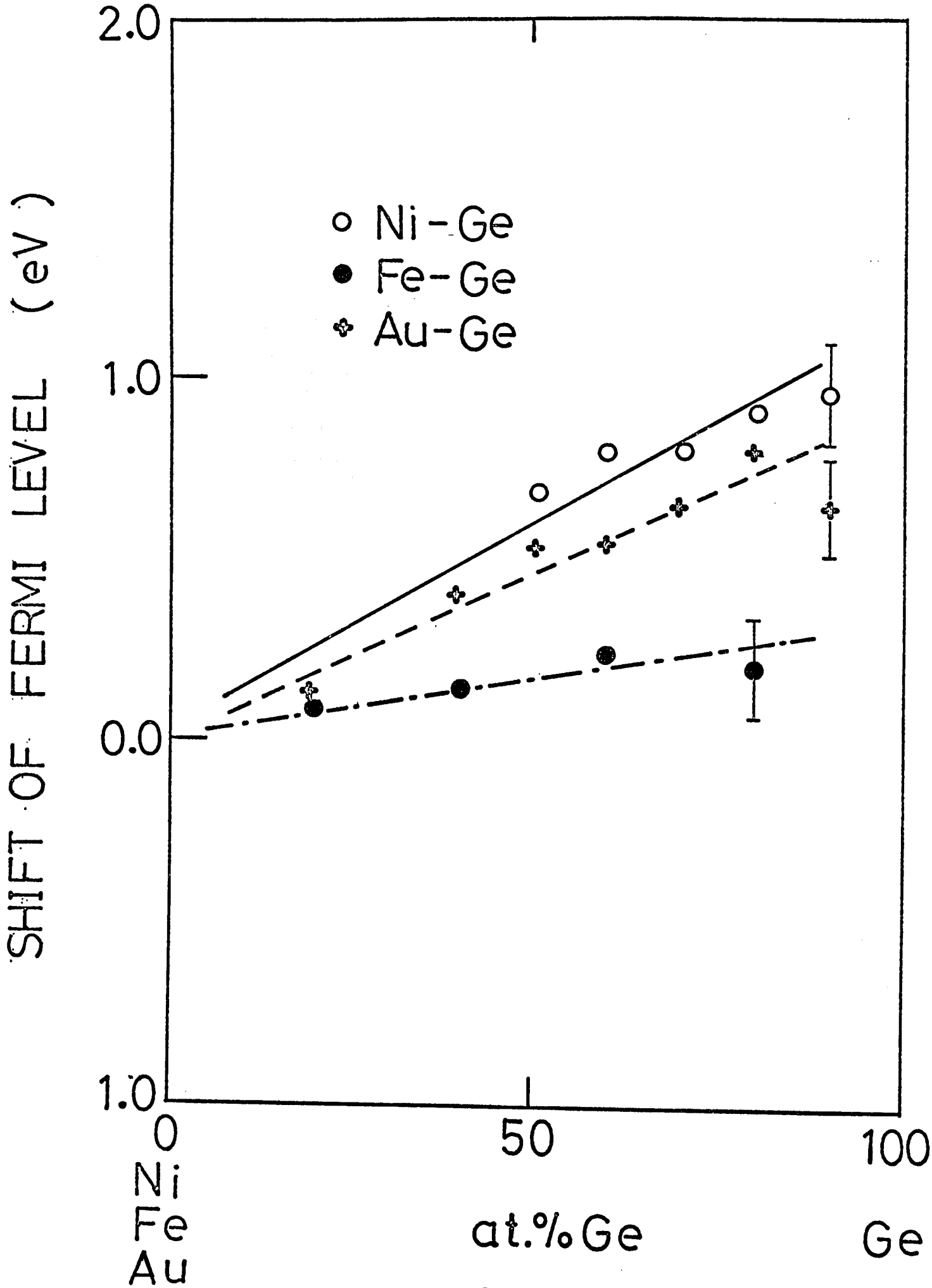
2.0
1.0
0.0
1.0
SHIFT OF FERMI LEVEL (eV)
Ni-Ge
Fe-Ge
Au-Ge
0
Ni
Fe
Au
50
100
at.% Ge
Ge

Fig 12

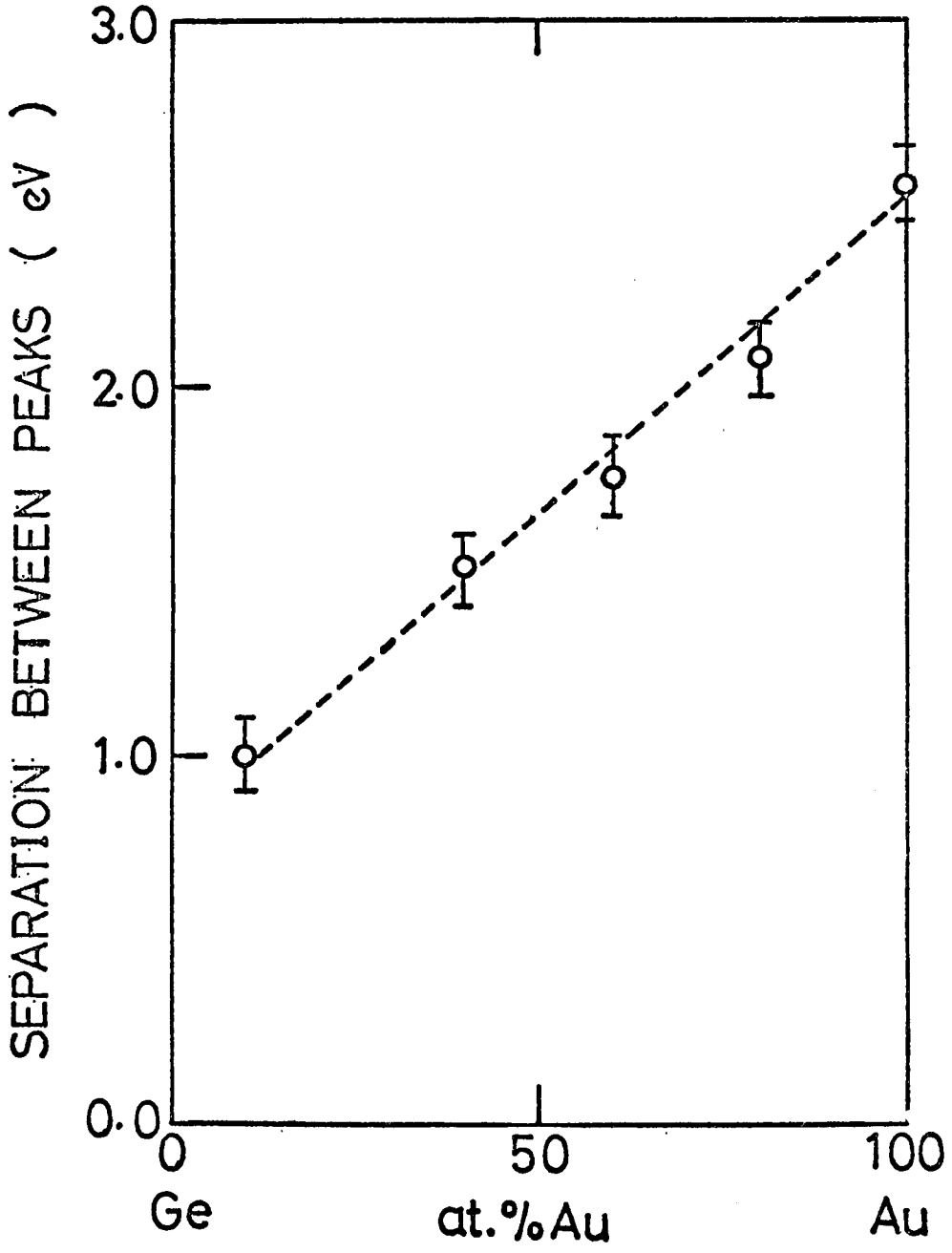

Fig. 13

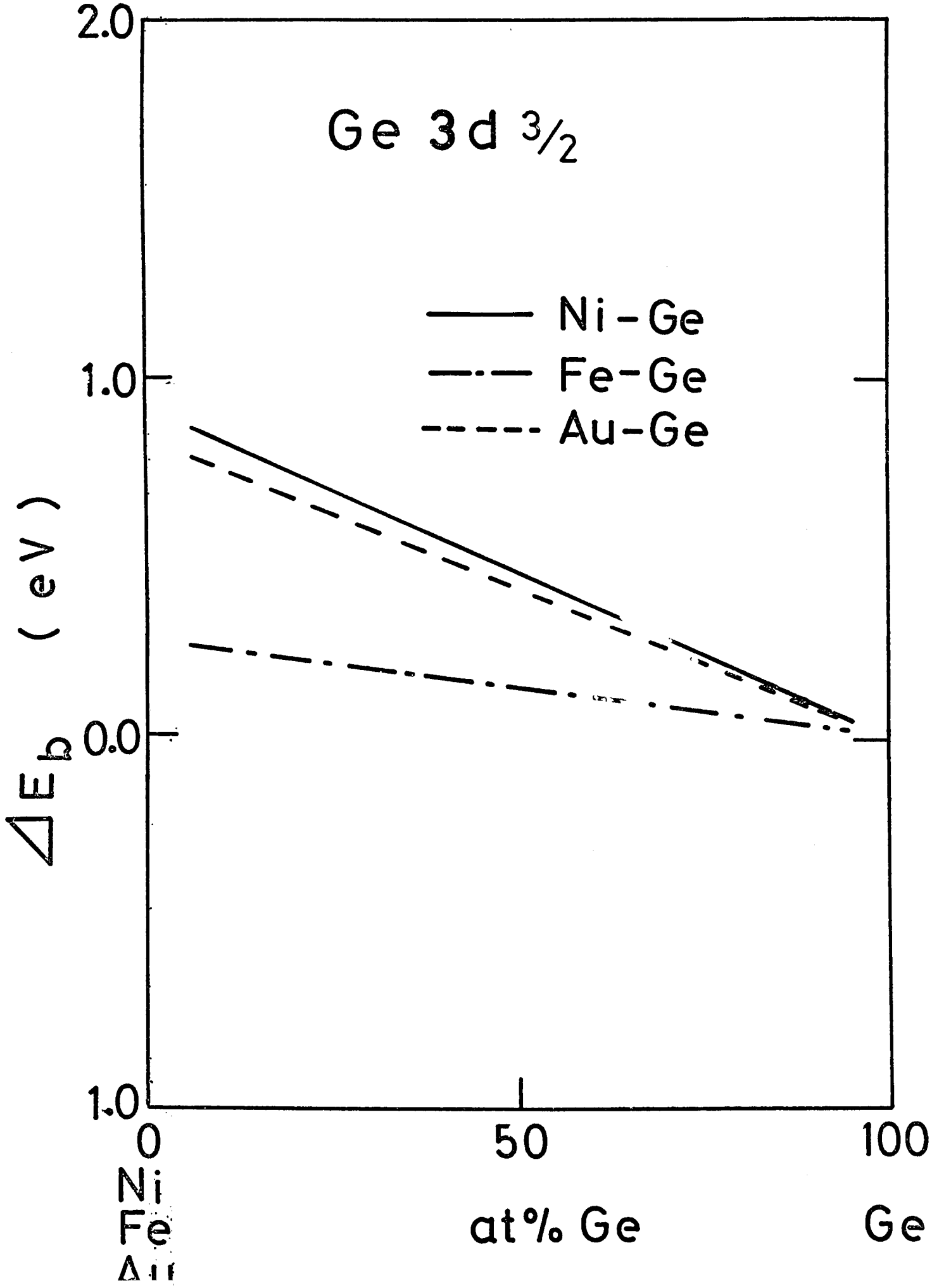

Acknowledgement

The author would like to acknowledge the contiuing guidance and encouragement of Professors H.Endo, T.Haseda, S,Minomuraand S.Ikeda.In preparing this presentation, the author had many discussions with his colleagues, Mr.J.Fukushima, Mr.O.Shimomura and Mr.K.Asaumi. Their contributions to this presentation have been very great and I take pleasure in acknowledging the important part played by them. The author was favored to have the assistance of Dr.K.Kishi who contributed his experimental skill and suggestion in the experiment of X-ray photoelectron emission. The author thanks to Professors M.Tanaka, M.Watabe and Dr.F.Yonezawa, Professor J.Kanamori and Dr.K.Terakura for many helpful discussions. Thanks are due to Mr.T.Ohtani, Mr.Ode, Dr.H.Okashita and also my colleagues in our laboratory. In the end I would like to express my thanks to Miss.M.Okamoto and my wife.